ornl

ORNL-6350

OAK RIDGE
NATIONAL
LABORATORY

MARTIN MARIETTA

Ultrasonic Techniques for the Evaluation of Ceramic Joints

W. A. Simpson, Jr.
R. W. McClung

OPERATED BY
MARTIN MARIETTA ENERGY SYSTEMS, INC.
FOR THE UNITED STATES
DEPARTMENT OF ENERGY

Printed in the United States of America. Available from
National Technical Information Service
U.S. Department of Commerce
5285 Port Royal Road, Springfield, Virginia 22161
NTIS price codes—Printed Copy: A04 Microfiche A01

Accession Number: 1959

Publication Date: Apr 01, 1987

Title: Ultrasonic Techniques for the Evaluation of Ceramic Joints

Personal Author: Simpson, W.A., Jr.; McClung, R.W.

Corporate Author Or Publisher: Oak Ridge National Laboratory, Oak Ridge, TN 37831 Report Number: ORNL-6350

Descriptors, Keywords: Ultrasonics Evaluation Ceramic Joint Bond Material Experiment Test NDE Structure Failure

Pages: 054

Cataloged Date: Oct 10, 1989

Contract Number: DE-AC05-84OR21400

Document Type: HC

Number of Copies In Library: 000001

Record ID: 20860

Source of Document: NTIS

ORNL-6350

Metals and Ceramics Division

ULTRASONIC TECHNIQUES FOR THE EVALUATION OF CERAMIC JOINTS

W. A. Simpson, Jr., and R. W. McClung

Date Published: April 1987

Prepared for the Assistant Secretary
for Conservation and Renewable Energy,
Office of Energy Utilization Research,
Energy Conversion and Utilization Technologies (ECUT) Program

Prepared by the
OAK RIDGE NATIONAL LABORATORY
Oak Ridge, Tennessee 37831
operated by
MARTIN MARIETTA ENERGY SYSTEMS, INC.
for the
U.S. DEPARTMENT OF ENERGY
under Contract DE-AC05-84OR21400

CONTENTS

ULTRASONIC TECHNIQUES FOR THE EVALUATION OF CERAMIC JOINTS*

W. A. Simpson, Jr., and R. W. McClung

ABSTRACT

The increasing use of structural ceramics in high-temperature applications has led to the need for nondestructive evaluation techniques to ensure the integrity of the ceramic materials and the quality of joints consisting of ceramics bonded to ceramics or to metals. We describe the development of ultrasonic techniques for the characterization of ceramic materials and for the detection of flaws in these materials and at ceramic joints. This work has led to the ability to determine which face of a 60-μm-thick layer of braze filler material is unbonded, thus providing information about the integrity of the ceramic–filler metal bond. We also describe the development of a rapid technique using Lamb waves to probe the bond between alumina coupons in flexure-strength specimens, whose geometry makes conventional ultrasonic evaluation of the bond difficult.

INTRODUCTION

The excellent high-temperature thermal, mechanical, and physical properties of structural ceramics make them likely choices for use in advanced engine designs to allow higher combustion temperatures and therefore higher thermodynamic efficiencies. In addition, the lower weight of such materials relative to that of high-temperature structural alloys should increase an engine's ratio of power to weight. Unfortunately, the low fracture toughness, and hence the small critical flaw size, of structural ceramics precludes the use of standard nondestructive evaluation (NDE) techniques that have been developed over the last 30 years for detection and characterization of critical flaws in metals. For example, flaws of critical size in most structural metals can be detected with ultrasonic waves whose frequencies lie in the range from 1 to 10 MHz. Consequently, most development in ultrasonics has encompassed this frequency range, with little activity occurring above 15 to 20 MHz. In conventional monolithic ceramics, however, the critical flaw size is about

*Research sponsored by the U.S. Department of Energy, Office of Energy Utilization Research, under the Energy Conversion and Utilization Technologies (ECUT) Materials Program, under contract DE-AC05-840R21400 with Martin Marietta Energy Systems, Inc.

20 μm, and for such small flaw sizes the use of frequencies of 50 MHz and higher is required. In addition, detection of such small flaws requires the use of focused radiation, and the propagation of such energy through the ceramic surface introduces severe aberration into the beam, thus limiting to a few millimeters the depth at which effective focus can be maintained. Finally, several heat engine designs require that a ceramic be joined to a metal to take advantage of the physical and/or mechanical properties of each. These applications require the development of technology for joining ceramics to other ceramics and to metals and, no less importantly, for inspecting such joints nondestructively to ensure bond integrity. This report describes work performed by the Nondestructive Testing Group of the Metals and Ceramics Division on the development of equipment and techniques for detecting small flaws in ceramic-ceramic and ceramic-metal joints.

The objective of this program is to investigate methods for NDE of ceramic joints leading to recommendations and development of techniques for evaluating important properties and characteristics that affect the serviceability of joints.

EXPERIMENTAL PROCEDURES AND RESULTS

CERAMIC MATERIALS

In order to develop techniques for the inspection of ceramic joints it is first necessary to characterize the ceramic materials themselves, since they will often be the determining factor in the choice of test parameters. This is in contrast to the ultrasonic inspection of metals, where the properties other than the wave velocities of the host can frequently be neglected. The engineering constants (Young's modulus, Poisson's ratio, etc.) can easily be determined nondestructively for ceramics by well-known techniques, but this information does not determine the basic inspectability of the sample for a given flaw size. For example, two specimens may have identical engineering constants, but one may be inspectable with 100-MHz ultrasonic energy while the second may not transmit energy above 20 MHz. This behavior results from the fact that

attenuation is highly sensitive to the microstructure of the host; for example, one can glean some information about the average grain size from an attenuation measurement. Therefore, to the determination of the standard engineering constants should be added the attenuation behavior of the particular specimen for ultrasonic energy in a frequency range commensurate with the flaw size of interest.

Transfer Curve

Although the measurement of attenuation at discrete frequencies is a standard procedure in ultrasonics, the use of such an approach at the high frequencies employed in ceramic inspection would be prohibitively expensive because of the high cost of transducers. A much better approach is to use a single broadband transducer to transmit a range of frequencies and, using a computer, to analyze each frequency component separately. This approach offers the additional advantage of automating the application of corrections to compensate for such nonspecimen losses as beam spread, acoustic impedance mismatch, etc. In addition, the effects of the transducer response and system electronics can be removed from the acquired data to yield a true attenuation versus frequency response for the specimen. This response is termed the transfer curve of the specimen, in analogy to the similar function in optics. In our work, all these corrections have been incorporated into a single computer program that computes the transfer curve from input data consisting of the signals reflected from the front and rear surfaces of a planar sample of the material under test.

When we first began computing transfer curves for ceramics, several anomalies arose that could not be attributed to the samples. In particular, the attenuation in all samples at frequencies above about 30 MHz was much higher than would be expected from optical measurements of the microstructure. This behavior was ultimately traced to the very thin (<1-μm) layer of water used to couple the ultrasonic energy into the ceramic part. For frequencies less than about 15 MHz, the thickness of this coupling layer is such a small fraction of the ultrasonic wavelength that it is negligible. As the frequency increases, however, the coupling layer becomes a larger fraction of a wavelength, and its presence is no longer negligible. When we analyzed this configuration, treating it as a

three-layer rather than a two-layer problem, it became obvious that a correction would have to be added to account for the presence of the coupling layer. Figure 1 shows how the reflection coefficient varies as a function of frequency for a water coupling layer 1 μm thick. At lower frequencies the coefficient approaches the two-layer value, where the effect of the water is negligible. Our computer program was subsequently modified to actually measure the thickness of the coupling layer during a test and provide a correction in the data. The transfer curve so obtained is now highly repeatable and in agreement with destructive analysis.

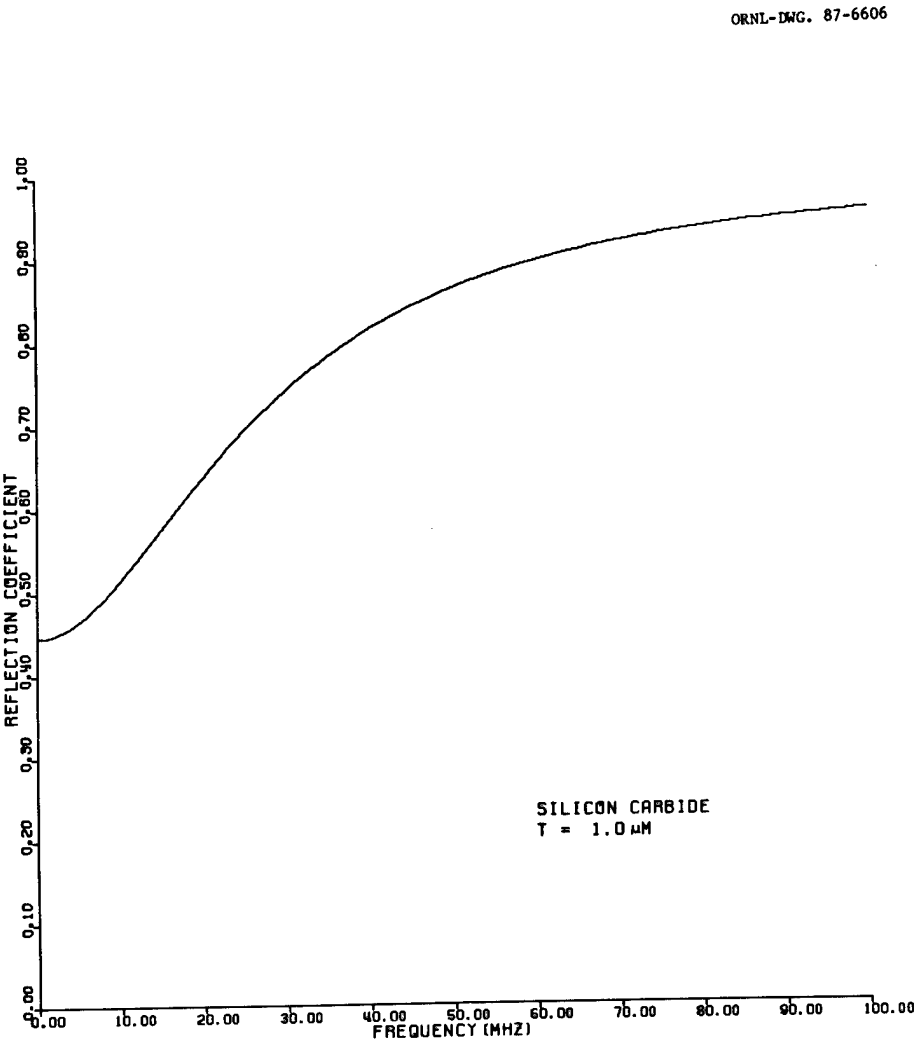

Fig. 1. Reflection coefficient at a water–silicon carbide interface for a 1-μm water layer.

Figures 2 and 3 illustrate the effect of the microstructure on the transfer curve. In Fig. 2, the sample is a piece of tetragonal zirconia polycrystalline (TZP) ceramic with a microstructure of primarily 10-μm tetragonal-phase grains. In Fig. 3, however, the sample is a partially stabilized zirconia (PSZ) with predominantly cubic grains about 100 μm in diameter. It is difficult to propagate through the PSZ an elastic wave whose frequency exceeds about 30 MHz because of severe scattering losses. For such material, the minimum detectable void diameter is probably also about 100 μm.

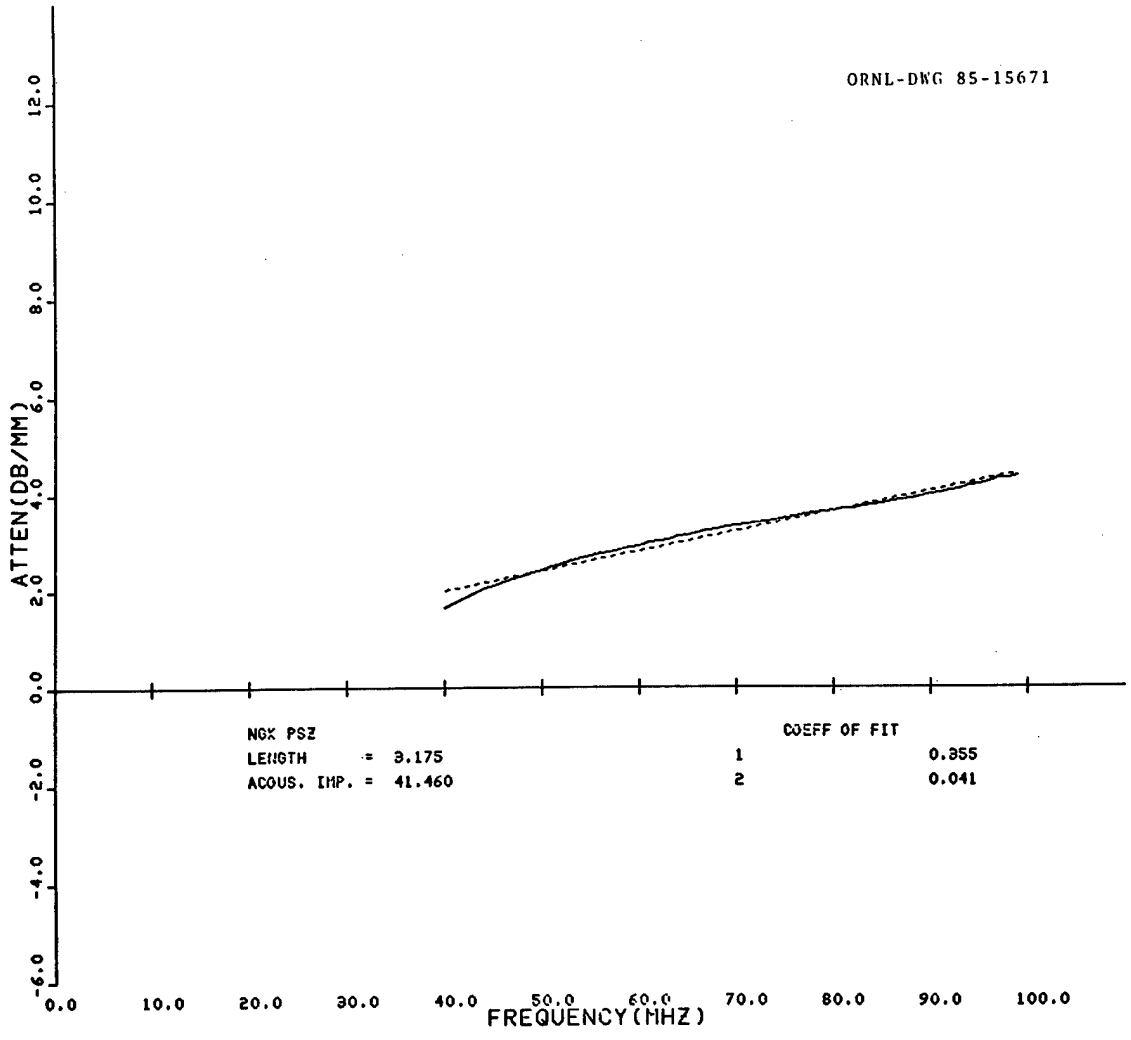

Fig. 2. Transfer curve of tetragonal zirconia polycrystalline ceramic.

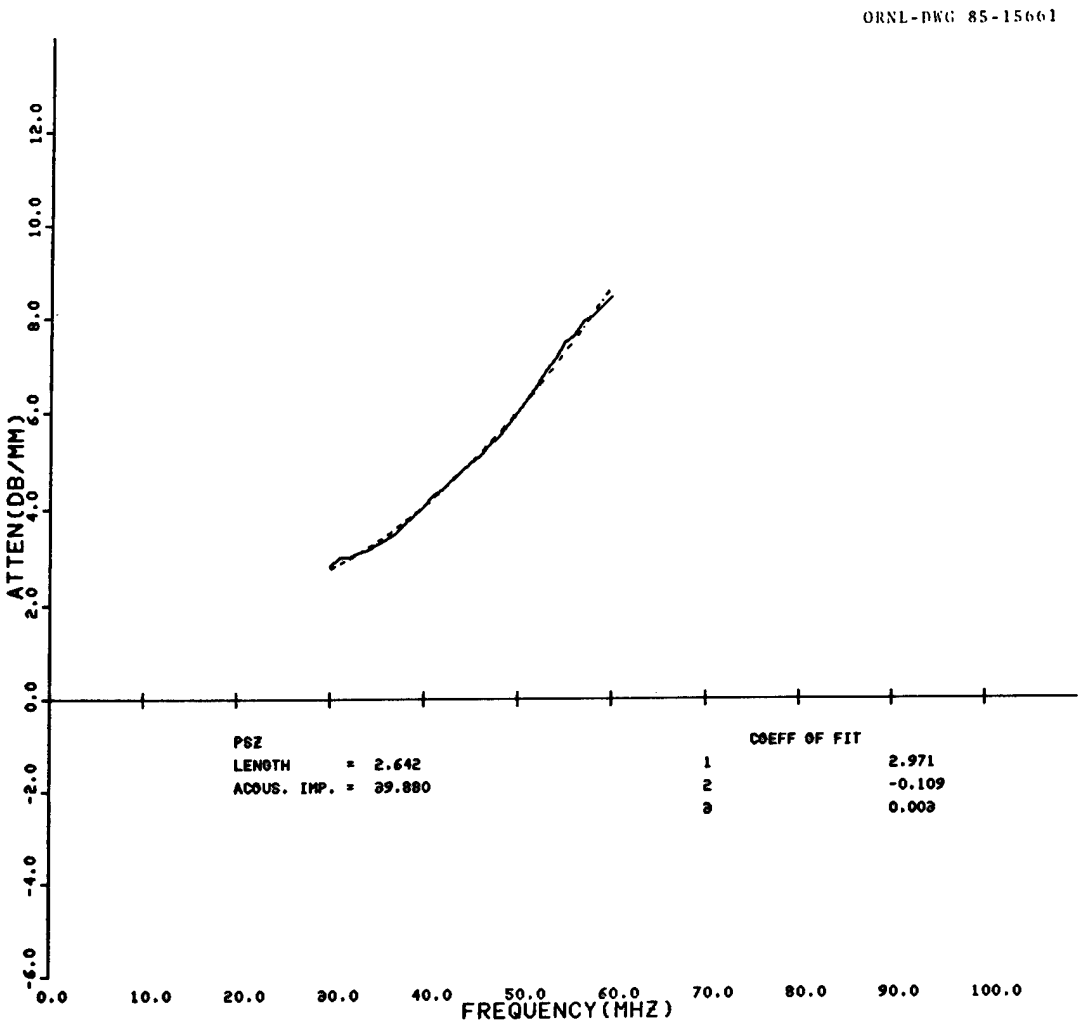

Fig. 3. Transfer curve of partially stabilized zirconia.

Detection of Flaws in Ceramics

Also of interest in characterizing the ultrasonic response of a ceramic material is the detection of flaws comparable to or larger than the critical flaw size, particularly if they occur in the vicinity of a joint. From published destructive analyses of flaw initiators in ceramic materials, a common flaw shape is the quasi-spherical void or inclusion. This is fortuitous, since a model exists for the scattering of elastic waves from spherical cavities and inclusions.[1] For a planar crack, we have previously demonstrated a successful model for measuring crack size.[2]

Figure 4 shows the calculated response to elastic waves of a spherical void in silicon nitride. The abscissa is the dimensionless product of the wave number, k (i.e., $2\pi/\lambda$, where λ is the ultrasonic wavelength in centimeters), of the incident radiation and the void radius, a. For a given flaw size, the abscissa is thus proportional to frequency. The ordinate is the differential scattering cross section. The response may be divided into three regions: (1) the low-frequency region (Rayleigh scattering) in which the scattering increases as the fourth power of the frequency, (2) the transition region (located at $ka \approx 1$), and (3) the high-frequency region in which the scattering cross section is oscillatory with an approximately constant average value. The latter behavior can be traced to interference between two waves scattered by the sphere. The first is the direct wave reflected from the near point of the sphere, and the second is the so-called "creeping" wave, which, after tangential incidence, propagates around the sphere and is reemitted after

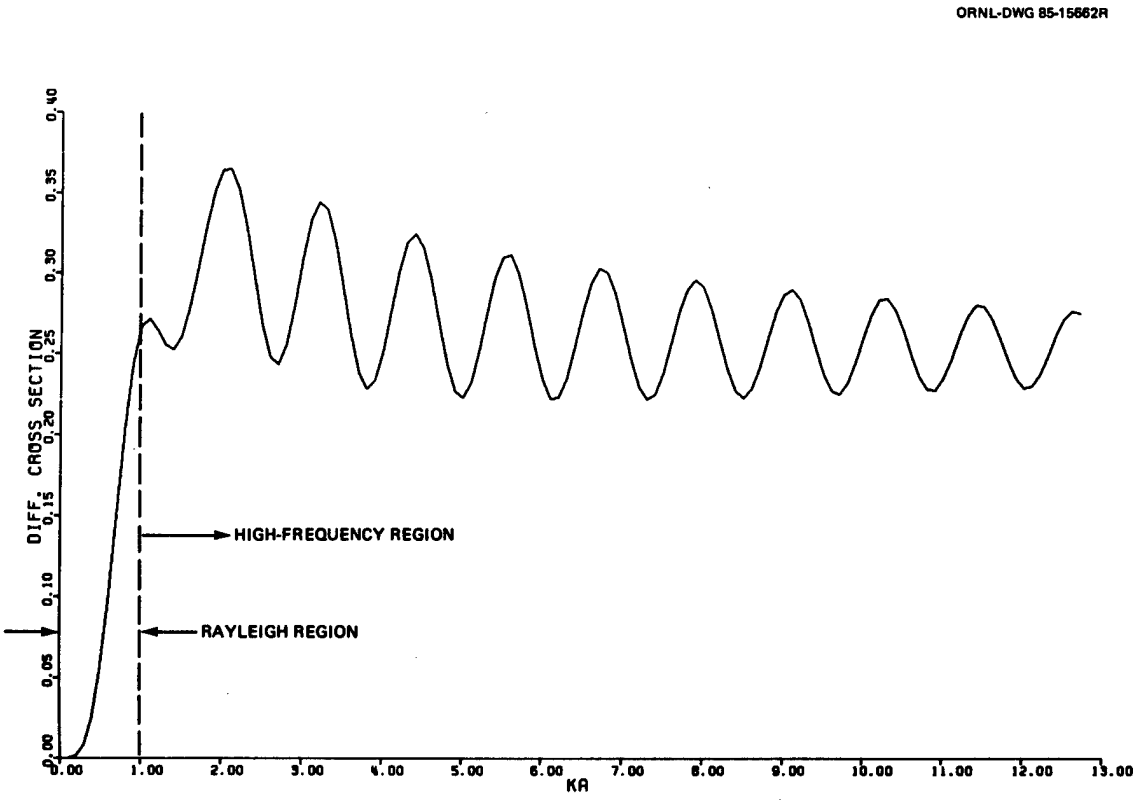

Fig. 4. Differential cross section for scattering from a spherical void.

traversing half the circumference. The periodicity of the oscillation is thus related to the size of the void. For natural flaws, however, even those whose shape is very nearly spherical, the surface roughness may rapidly attenuate the latter wave, and the high-frequency scattering depicted in Fig. 4 may be replaced by a near-constant value. In this case, the size of the scattering center may be approximated by noting that the transition region occurs at $ka \approx 1$; thus if the frequency of the turning point, that is, the transition from Rayleigh to high-frequency scattering, is known, the radius of the sphere may be estimated.

Figure 5 shows experimental data obtained on a natural flaw in TZP ceramic. Here the turning point occurs at about 89 MHz. Based on the measured velocity, the flaw diameter was estimated to be approximately 25 μm. That the flaw size is of this order of magnitude is also supported by the fact that it could not be detected reliably with a scan increment of 50 μm but could with an increment of 25 μm.

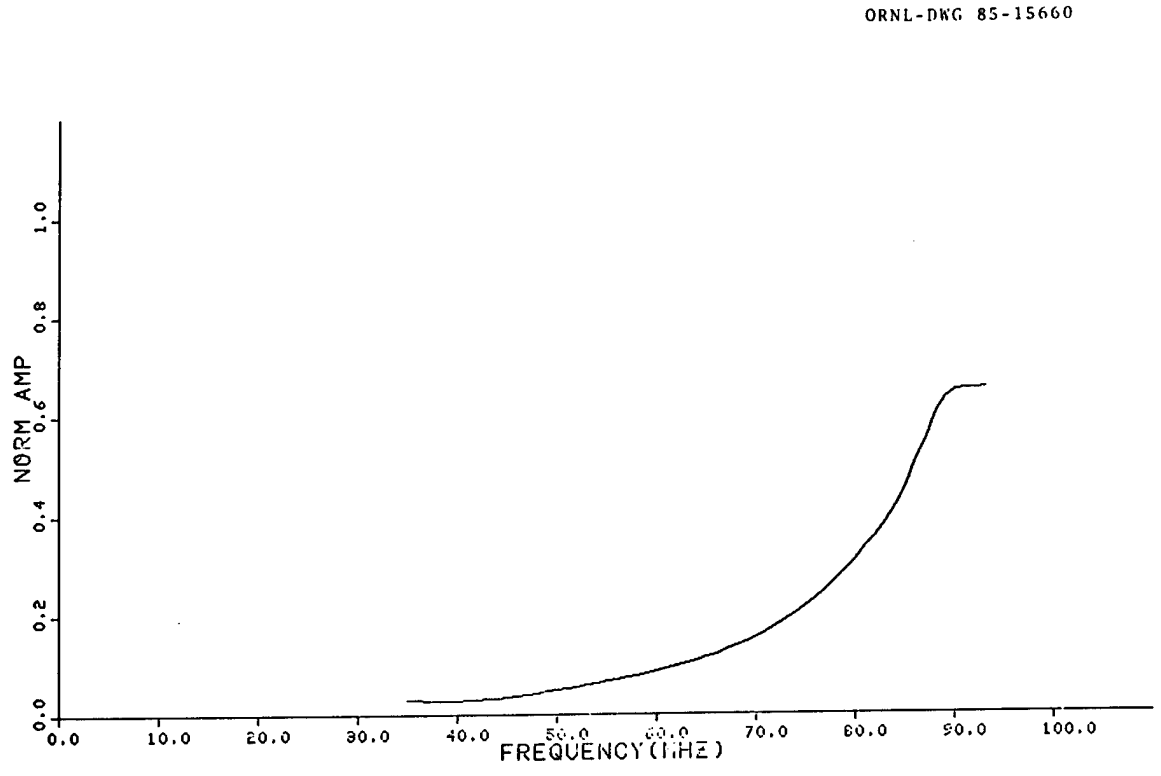

Fig. 5. Experimental data for scattering from a natural flaw in tetragonal zirconia polycrystalline ceramic.

PLANAR JOINTS

Ceramic-Cap Piston Specimens

Two large ceramic-to-metal brazements that mock up the attachment of a ceramic cap to a diesel engine piston were made available for nondestructive testing studies. These specimens are 111 mm (4 3/8 in.) in diameter and consist of a 6.4-mm-thick (0.25-in.) PSZ cap brazed to a nodular cast iron (NCI) disk via a titanium transition piece and a commercial Ag-Cu-Sn brazing filler metal.[3] The surface of the ceramic had been vapor coated with titanium to promote wetting by the filler metal. Figure 6 shows the geometry of the joint and Fig. 7 one of the specimens. The thickness of each braze layer was about 60 μm and that of the titanium transition piece about 0.6 mm.

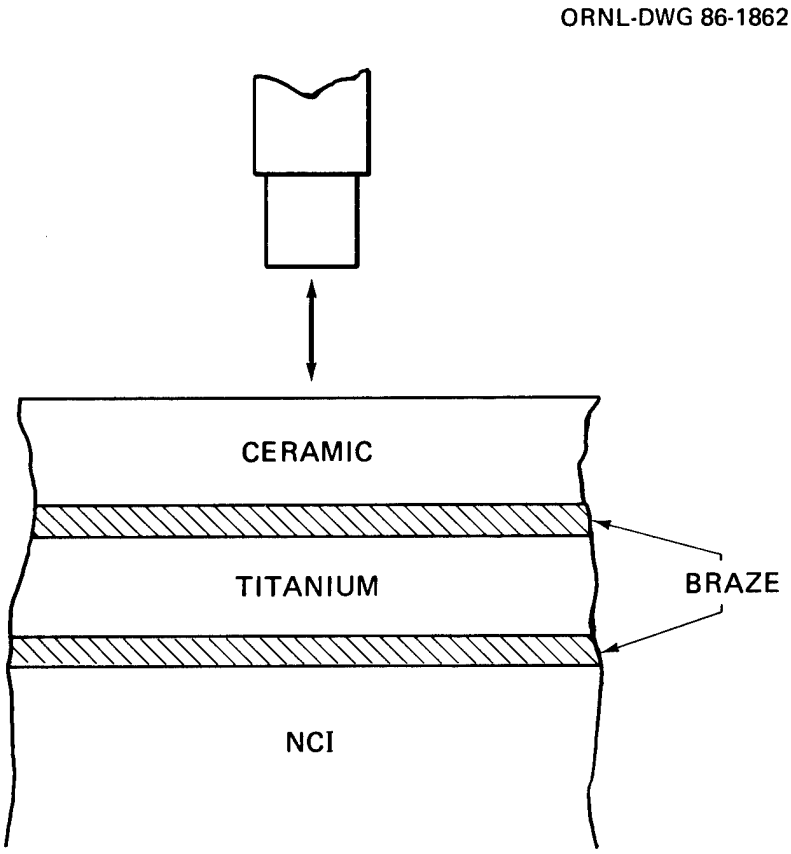

Fig. 6. Diagram of a transition joint for bonding a ceramic to nodular cast iron (NCI) to simulate a diesel-engine piston with a ceramic cap.

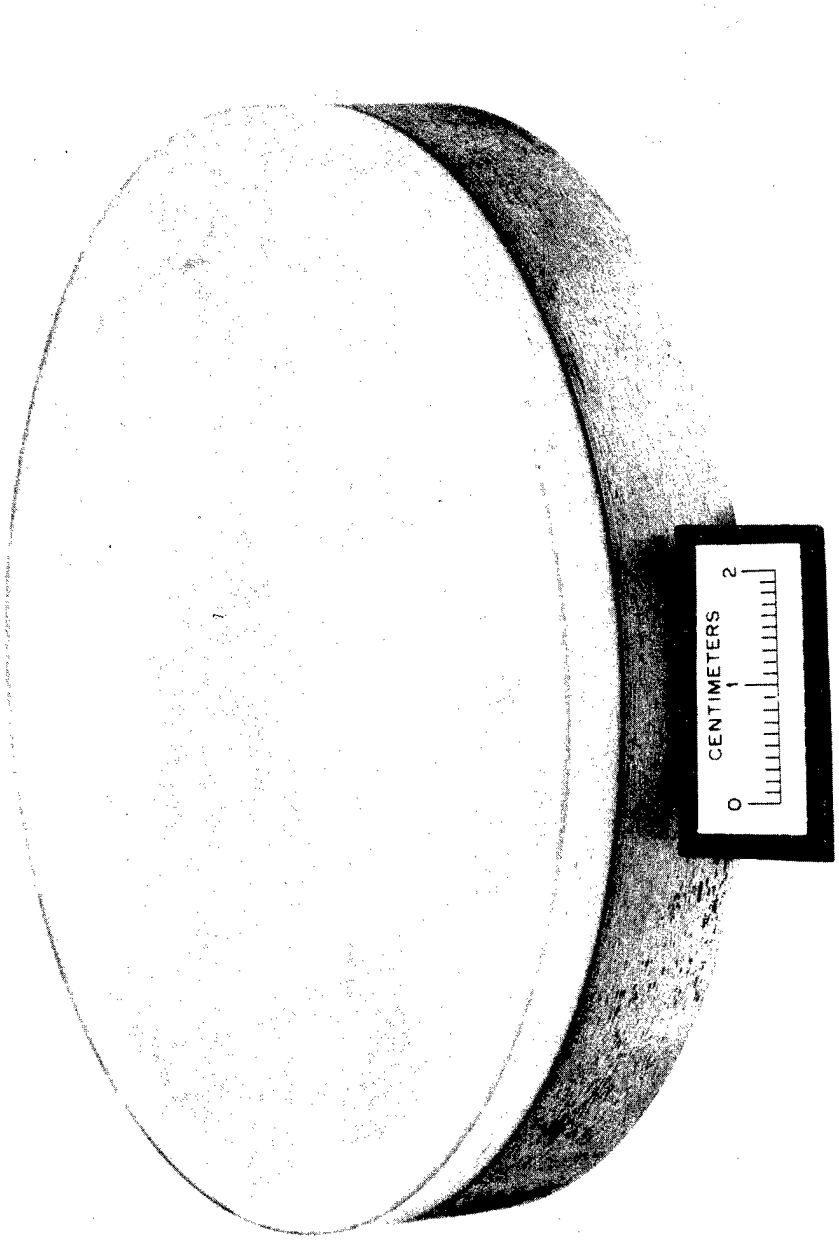

Fig. 7. Ceramic-cap diesel-engine piston specimen (one of two).

Initial ultrasonic examination of each specimen indicated a relatively high attenuation for elastic waves in the ceramic cap, restricting the maximum usable frequency to about 25 MHz. From our previous studies of the attenuation characteristics of PSZ material, this behavior was consistent with the scattering losses produced by the relatively large grain size (≈100 μm) of this ceramic.

Both specimens were scanned in our high-frequency (100-MHz) ultrasonic system, which permits variations in the transmission of the ceramic-metal bond to be displayed as a gray-scale image. A flat (unfocused), broadband transducer was used, and both samples were found to contain nonbonded regions near the center. Figure 8 shows the result for one of the brazements. Here lighter areas indicate relatively better transmission through (less reflection from) the bond, and darker areas indicate relatively poorer transition (greater reflection). The dark area near the center is completely unbonded. (In the original data this area was uniformly dark; it did not reproduce well photographically, however.) The dark ring near the periphery of the sample is an edge effect caused by the unfocused transducer.

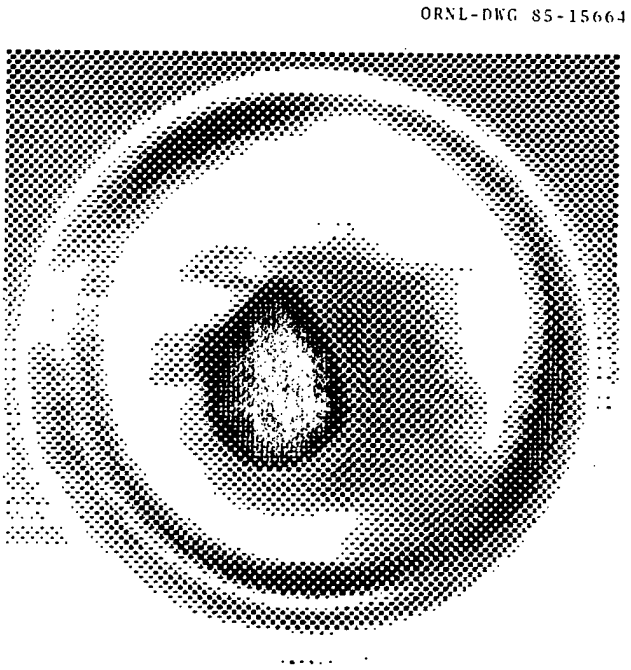

Fig. 8. Gray-scale presentation of ultrasonic transmission through the bond in piston specimen 1.

The samples were scanned a second time using a focused transducer. Focusing minimizes edge effects and more sharply delineates the region of unbond. Figure 9 shows the raw gray-scale data for the second sample, which is seen to be unbonded in the center and at several locations around the periphery.

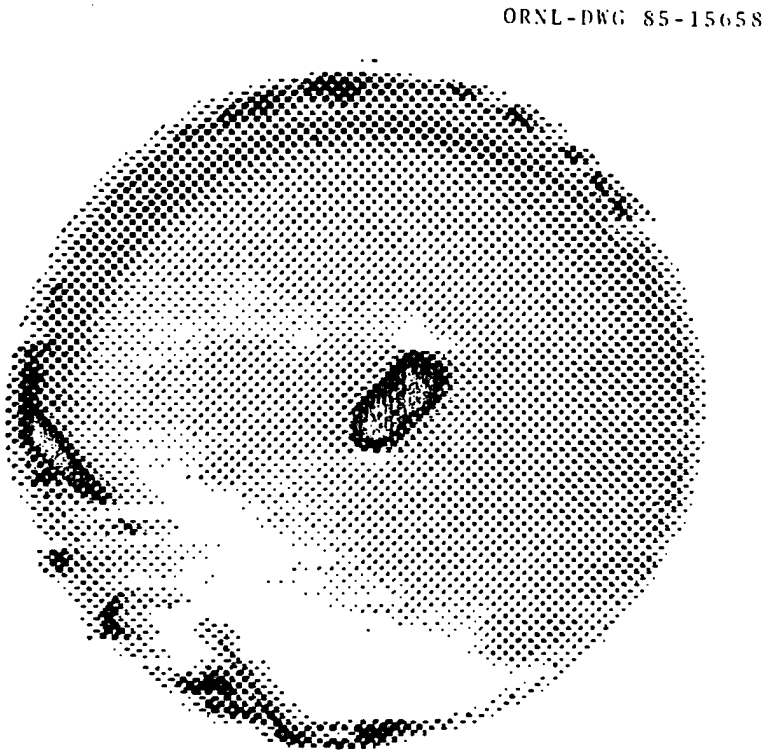

Fig. 9. Gray-scale presentation of ultrasonic transmission through the bond in piston specimen 2.

The raw pixel data from these gray-scale images were next computer processed to permit expansion of a selected range of gray-scale values. Such processing allows minor (<3-dB) bond variations to be ignored and fluctuations within the unbonded areas to be enhanced. Figures 10 and 11 show the processed images for the two specimens. As expected, the areas delineated show virtually no variations, which is indicative of complete unbonding. The shape, size, and location of the affected areas are also precisely determined by this processing.

ORNL-DWG 85-15657

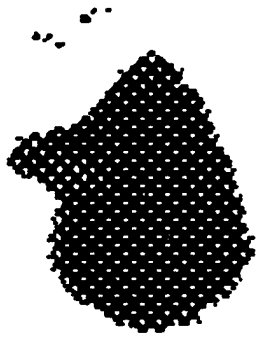

Fig. 10. Enhanced gray-scale presentation of ultrasonic transmission through the bond in piston specimen 1.

ORNL-DWG 85-15659

Fig. 11. Enhanced gray-scale presentation of ultrasonic transmission through the bond in piston specimen 2.

Because there are several interfaces in the PSZ-NCI joint (Fig. 6), one would like to know at which of these interfaces the unbond occurs, since this information could provide insight into the origin of the problem. In addition, while the precise location of the unbond may be immaterial from an accept-reject point of view, such information is important in the development of ceramic brazing technology. For example, if the unbond occurs at the ceramic-braze interface, it could indicate a failure of the braze filler metal to wet the ceramic surface, and wettability is a major consideration of the brazing development program. Fortunately, the location of the unbond can be determined nondestructively from the ultrasonic scattering data. Figure 12 shows the rf waveform of signals scattered by the transition joint in three areas of the specimen whose data were shown in Figs. 9 and 11. In Fig. 12, the upper trace (trace A) is that obtained from a well-bonded region. The two signals are from the faces of the 600-μm-thick titanium transition piece, with the PSZ to the left and NCI to the right. The ultrasonic wave is incident from the PSZ. In trace B, the second signal is much larger, and the third signal, resulting from reverberation in the titanium, indicates that the unbond occurs on the NCI side of the titanium. In trace C, the first signal is much larger, and the absence of the signal from the opposite face of the titanium indicates that the sample is unbonded on the PSZ side of the titanium.

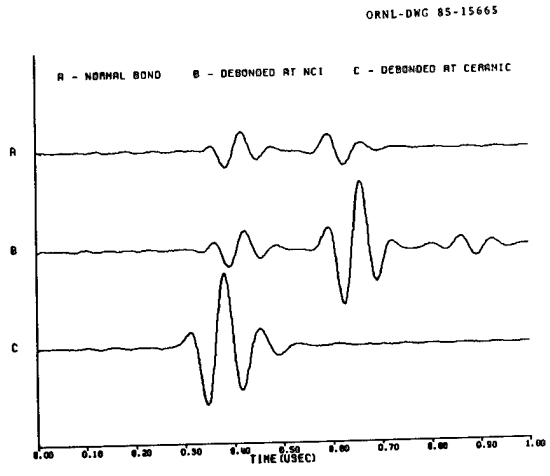

Fig. 12. Radio-frequency waveform of the ultrasonic signal scattered by the interface of piston specimen 2 for various bond conditions.

If the ceramic material will support elastic waves of a sufficiently high frequency, the signals from opposite faces of the nominal 60-μm-thick braze layer can be resolved (a time resolution of only 30 ns), and it is then possible to tell directly whether the unbond occurs at the ceramic-braze or braze-titanium interface. For example, Fig. 13 shows the waveform obtained from the joint region of a sample containing TZP (wide bandwidth) ceramic. The first two signals originate at the faces of the nominal 60-μm-thick braze layer between the TZP and the titanium transition piece. The second two are from the similar braze layer between the titanium and the NCI substrate. Note that the signals from the braze layers are resolved, which permits the condition of any of the four interfaces to be monitored. The restricted bandwidth of the PSZ is not sufficient to resolve these signals (frequencies above about 30 MHz are not transmitted). However, we have recently developed a technique to enhance the resolution of closely spaced ultrasonic signals.[4] Use of this technique will generally produce delta functions in the output data at the location of each individual wave center in the input data, even when the waves are too closely spaced to resolve in the time domain. When this technique was used to process the signals from the data of Fig. 12, the signals from either face of the braze layers could be resolved, as shown in Fig. 14. Since all four signals are present, the region is one in which the sample is well bonded. For the central unbond region of the simulator shown in Fig. 11, however, the processed data show only a single

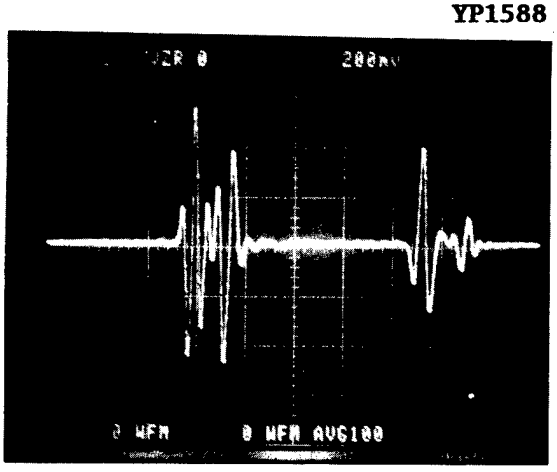

Fig. 13. Radio-frequency waveform of the ultrasonic signal scattered by the interface in tetragonal zirconia polycrystalline ceramic.

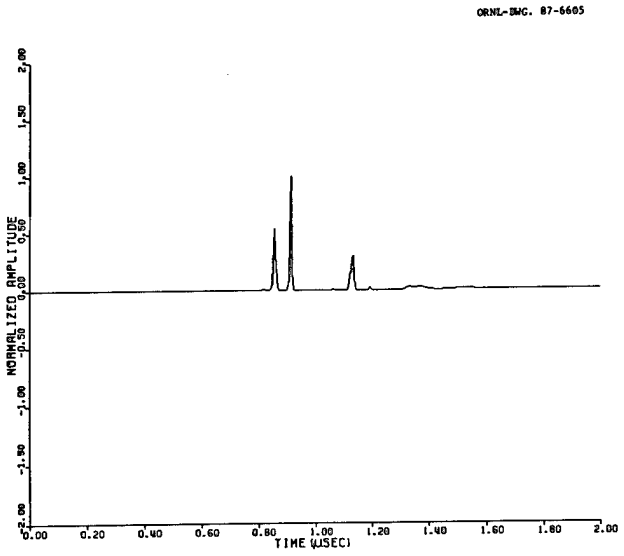

Fig 14. Processed data showing recovery of four interface signals in the bonded region of tetragonal zirconia polycrystalline ceramic.

delta function at the location of the PSZ-braze interface, indicating that the problem is failure of the braze to adhere to the ceramic.

These results indicate that for both samples, the central unbond occurs at the PSZ interface. For the specimen of Figs. 9 and 11, some of the edge indications are unbonded at the PSZ interface and some at the NCI interface.

Following NDE, the Materials Joining Group sectioned the sample of Figs. 9 and 11 through the unbonded region delineated by the central indication. When the region was cut out, the ceramic cap actually fell off. Subsequent metallographic examination of the ceramic-braze interface revealed the presence of extreme porosity, possibly due to trapped gas. The nondestructive results were thus validated.

Shear Specimens

Following examination of the piston-cap specimens, some smaller ceramic-metal brazements were made available. These samples were approximately 9-mm-square pieces of 3.5-mm-thick zirconia ceramic brazed to an NCI substrate with a 0.6-mm-thick titanium transition piece. In this case, however, the ceramic was a fine-grained TZP material that could support elastic waves at frequencies in excess of 100 MHz. In such

samples, effective focus could be maintained at depths up to 5 mm for these frequencies: accordingly, a 100-MHz focused transducer with a focal length of 25.4 mm in water was obtained to exploit this condition. At this frequency and with the transducer focused at the PSZ-braze interface, the signals from either side of the 60-μm braze layer could be resolved, even though these signals are separated by only about 30 ns. Therefore, we were able to gate selectively the signal from the TZP-braze interface for analysis. This signal is an indicator of the quality of the bond that exists between the braze filler metal and the TZP. Figure 15 shows two of the samples and Fig. 16 the results of scanning the bond region. In these gray-scale presentations, lighter areas indicate relatively better bonding while darker regions depict relatively poorer bonding. The sample on the right has numerous small regions where there is lack of bonding. These regions average perhaps 100 μm in diameter and are probably caused by bubbles of trapped gas in the braze material. The presence of these bubbles has been previously demonstrated by destructive analysis and inferred from examination of the fracture surface, but, until now, we have not been able to detect their presence nondestructively.

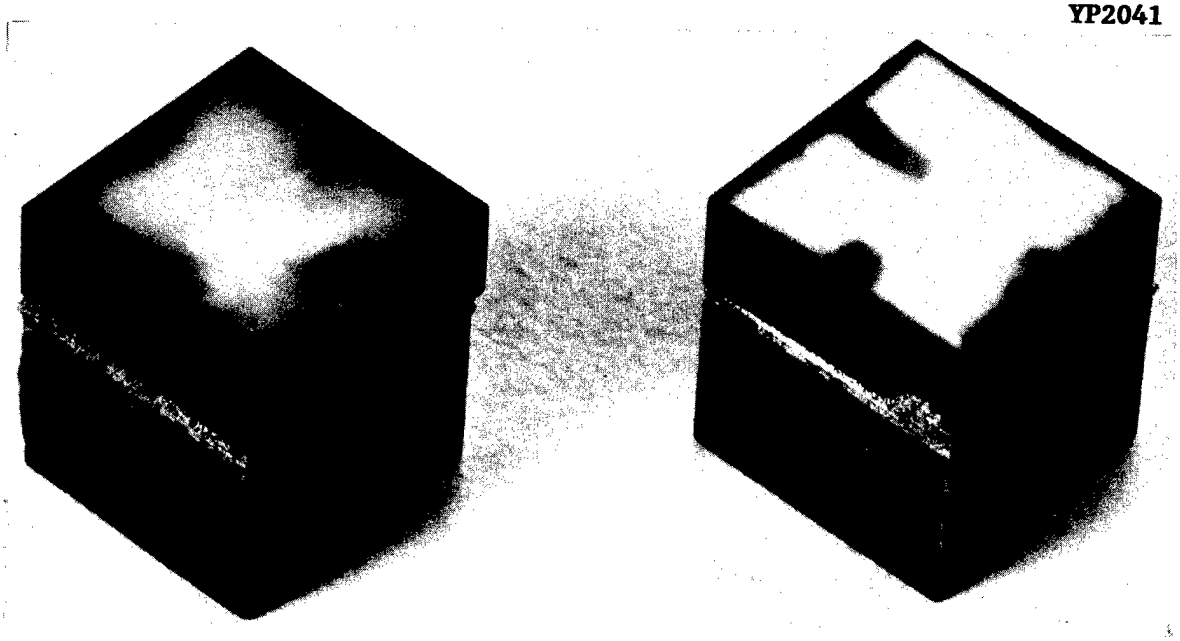

Fig. 15. Tetragonal zirconia polycrystalline ceramic joint specimens.

ORNL-Photo 1849-86

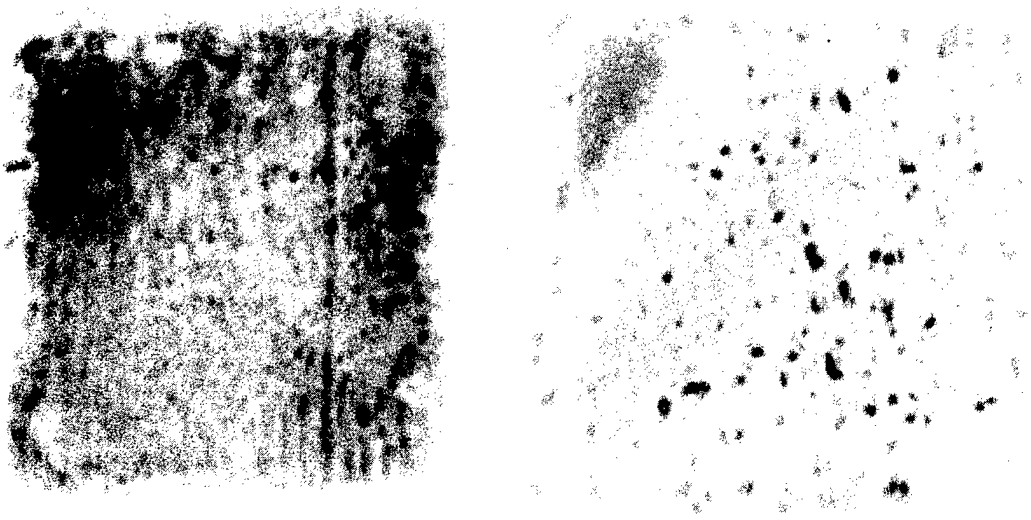

Fig. 16. Gray-scale presentation showing the detection of pores in the braze layers of the ceramic joint specimens shown in Fig. 15.

A diagonal band, running from lower left to upper right of the sample on the right, can be seen in the data of Fig. 16. The cause of this darkening is not known, but possibilities include the presence of microporosity or residual stress in the braze layer. The dark area in the upper left of the sample on the right is caused by severe thinning of the braze material.

The generally darker nature of the sample on the left in Fig. 16 is possibly attributable to use of a different grade of ceramic. Small variations in the acoustic properties alter the reflection coefficient at the TZP-braze interface and vary the average brightness of the reproduced data.

The sample on the left also exhibits a periodic variation in the interface that may be caused by machining marks on the TZP. No such marks are detectable on the visible surface, but they sometimes occur on one or more surfaces of the blanks.

The above results indicate that a great deal of information about the nature of the PSZ-braze bond can be gleaned from the ultrasonic scattering if the signals from the braze layer can be resolved. However, if they cannot, as is the case at typical ultrasonic frequencies (1–10 MHz), the signal generated by subtle variations at the filler metal–PSZ interface will be swamped by the signals from the filler metal–titanium interface.

Manufactured Flaws

We have considerable interest in determining the minimum detectable area of unbond in a ceramic joint. From the backscattering spectrum obtained from discrete flaws in ceramics, we earlier showed (see Fig. 5) the ability to infer a minimum measurable flaw size of about 25 μm (the minimum detectable flaw size will be still smaller) with our present system. It is difficult to fabricate discontinuities in this size range. However, we obtained a standard consisting of a bonded couple between a P-leg and an N-leg of a silicon-germanium thermoelectric sample. The bond contains three manufactured flaws having diameters of 250, 650, and 125 μm, and the acoustic properties (i.e., velocity and density) of the silicon-germanium are similar to those of typical ceramics. Figure 17

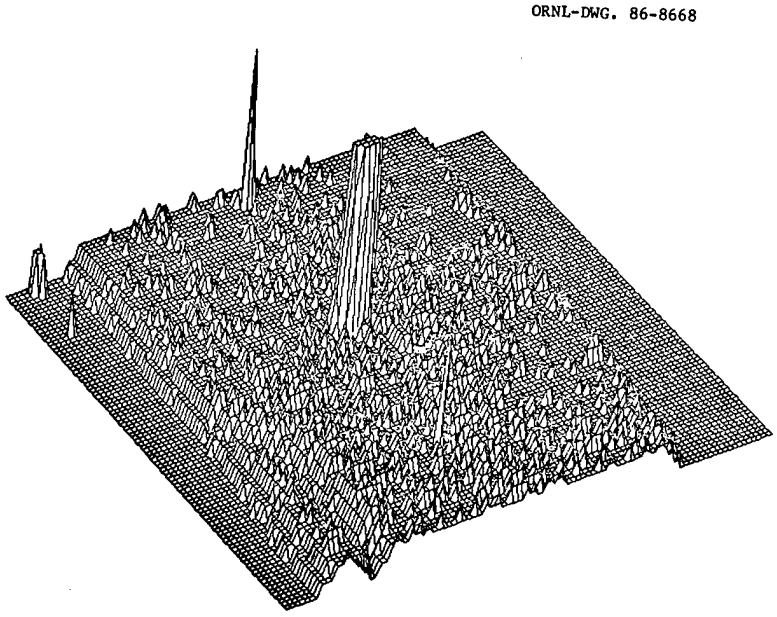

Fig. 17. Three-dimensional presentation of the ultrasonic detection of, left to right, 250-, 635-, and 125-μm flaws at the interface between two silicon-germanium thermoelectric samples.

is a pseudo three-dimensional view of the ultrasonic scattering from the bond line showing the detection of all three flaws. In the lower left of the figure is a natural crack that extended through the substrate and terminated at the interface. Figure 18 is a view of the data from a lower angle, making the smallest flaw more visible. Figure 19 is an expansion of the region around the 125-μm flaw. Note that the flaw signal is much larger than the background from the interface; thus, we should be able to see flaws considerably smaller than 125 μm reliably.

ORNL-DWG. 86-8669

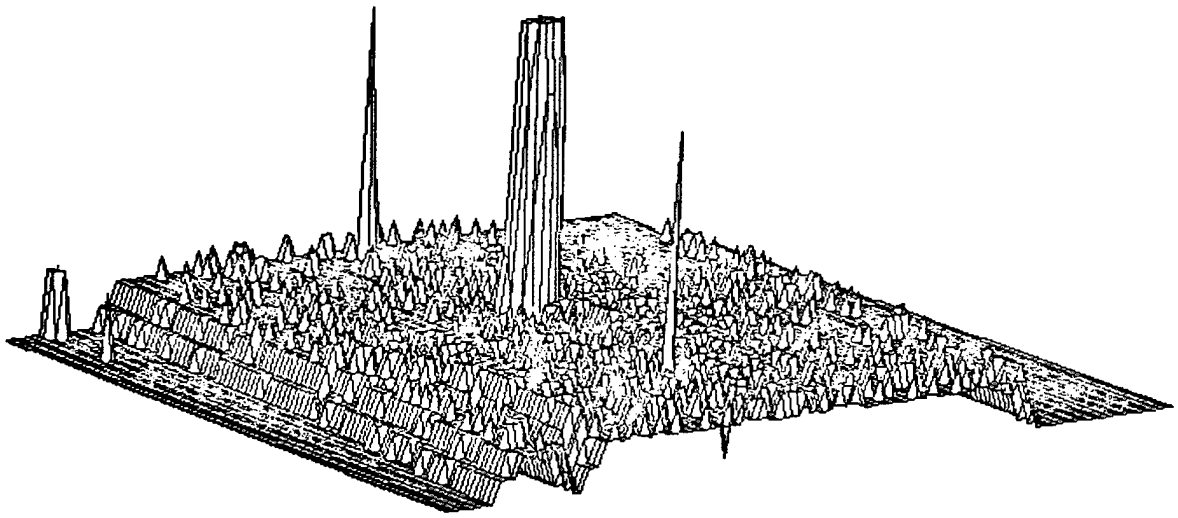

Fig. 18. Three-dimensional presentation (from a lower angle then in Fig. 17) of the ultrasonic detection of, left to right, 250-, 635-, and 125-μm flaws at the interface between the two silicon-germanium thermoelectric samples.

ORNL-DWG. 86-8671

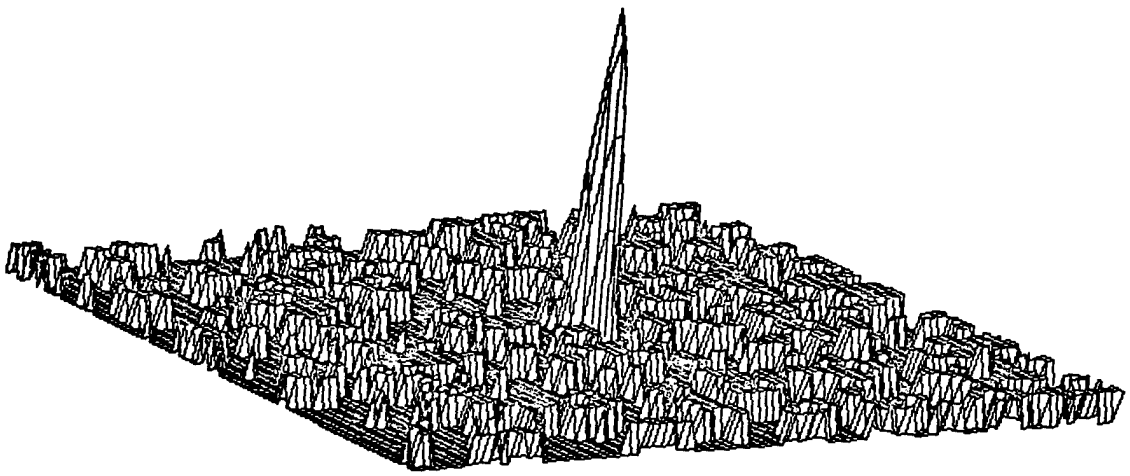

Fig. 19. Three-dimensional presentation of the region around the 125-μm flaw at the interface between the two silicon-germanium thermoelectric samples.

BUTT JOINTS

Lamb Wave Studies

For the samples described earlier in this report, the specimen geometry was such that bulk-wave probing of the joint region (albeit at frequencies far above those used in conventional ultrasonic testing) could be performed at normal incidence. We demonstrated earlier the ability to resolve signals from either side of the 60-μm-thick layer of brazing filler metal when the ultrasonic waves were incident normally on the joint. This capability then allowed us to determine whether a lack of bond occurred at the ceramic or metal interface of the joint and to measure the variation in filler metal thickness across the specimen.

For some specimen configurations, normal-incidence testing of the braze region using bulk waves is not possible. For example, a butt-braze joint between thin plates requires angle beams if bulk waves are used to interrogate the interface. While this configuration may or may not be important in the final application of ceramic joining to heat engines, it is of considerable importance to the development of joining technology in that many test specimens use such joint geometries. For example, specimens to measure flexural strength of ceramic-ceramic or ceramic-metal brazements are of this type (see Fig. 20), and inspection techniques must be developed so that correlations between NDE indications and mechanical properties can be determined. Only in this way can one differentiate between significant and ignorable indications.

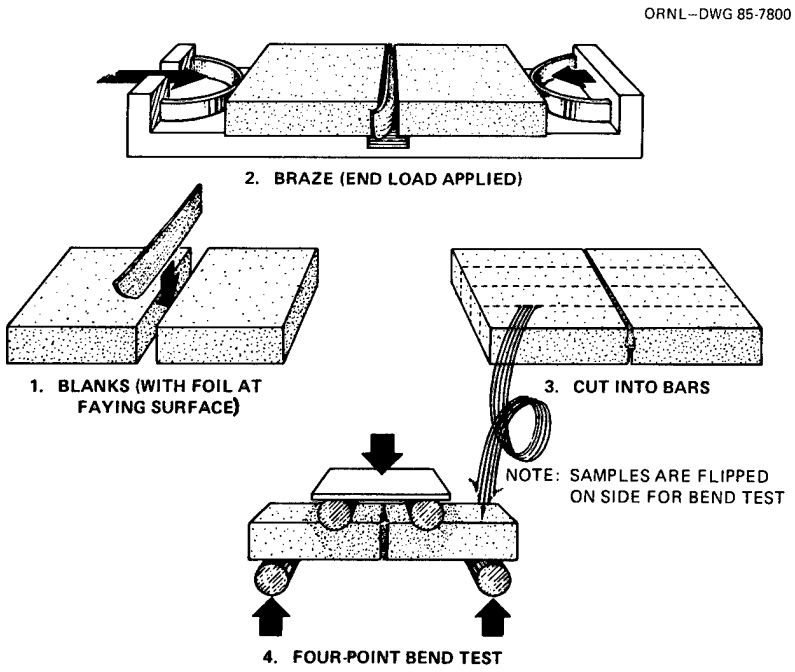

Fig. 20. Fabrication of ceramic flexure-strength specimens with butt-braze joints.

We have examined several butt-braze joints in 25.4 × 14.2 × 2.9 mm alumina coupons using high-frequency angle-beam techniques. While this approach would appear to have considerable potential for evaluating bond quality, the results thus far have been more difficult to interpret than the results from normal-incidence tests, and they suffer from the fact that the focal point of the transducer cannot be maintained exactly on the bond across the full height of the joint. This test is also relatively slow, since the bond must be scanned using a small linear increment.

A second approach for evaluating bond quality in butt-joint specimens relies on measurement of the transmission coefficient of so-called plate or Lamb waves propagated through the bond. In this technique, a Lamb wave, which is the elastomechanical analog of guided electromagnetic waves, is excited on one side of the joint and the amplitude of the wave on the second side measured after propagation through the bond. This approach has the advantage of requiring scanning only along a single axis, making it much faster than conventional testing. The frequencies involved are also quite low, typically 1 to 5 MHz. The quantity determined by this measurement is the relative area of the bonded region, which has been related to the prediction of shear strength for spot welds in metals.[5]

As is the case for electromagnetic guided waves, Lamb waves are highly dispersive. Since the propagation of such a wave along a plate produces (microscopic) flexure of the plate, Lamb waves can produce either symmetric or antisymmetric modes according to the symmetry of the flexure with respect to the center line of the plate. Figures 21 and 22 show the calculated dispersion curves for the first four symmetric and antisymmetric modes in 2.9-mm-thick alumina. Since the ordinate gives the Lamb wave phase velocity (normalized by the shear wave velocity), it is also related to the angle of incidence necessary to generate the given Lamb mode. Thus a horizontal line will intersect the various possible modes, whose abscissas give the frequencies necessary to establish the modes at the indicated angle of incidence of the exciting energy.

ORNL-DWG. 86-8672

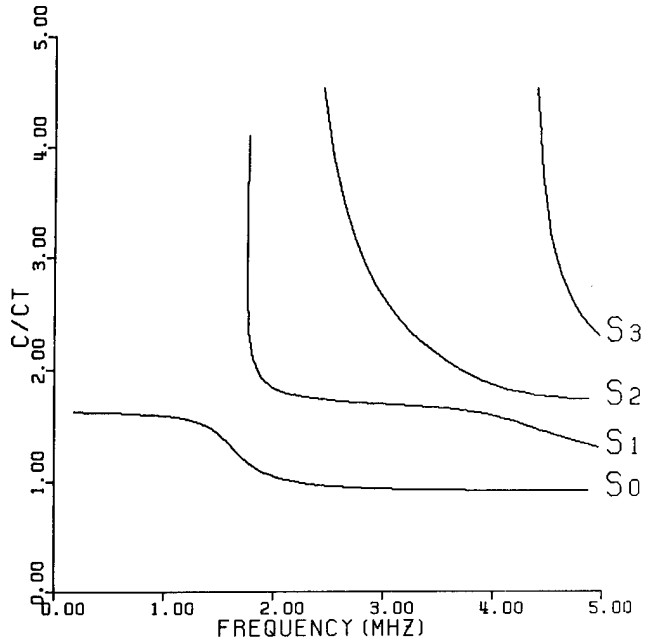

Fig. 21. Dispersion curves for symmetric Lamb wave modes in alumina.

ORNL-DWG. 86-8673

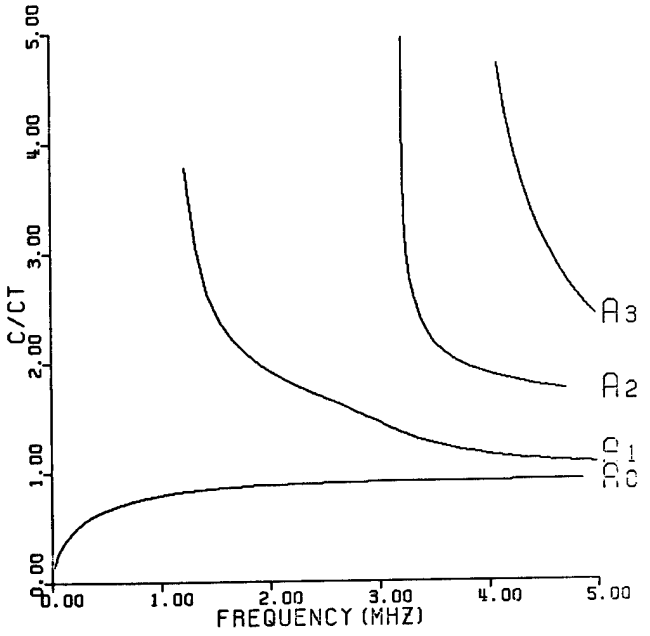

Fig. 22. Dispersion curves for antisymmetric Lamb wave modes in alumina.

Figure 23 is an experimental result showing the excitation of five Lamb wave modes in a 2.9-mm-thick alumina coupon. The normalized velocity of each wave is 1.25, and the mode frequencies are in good agreement with the values shown in Figs. 21 and 22. Note that this normalized velocity does not intersect the dispersion curve of the lowest-order antisymmetric mode; thus, this wave is not present in the spectrum. The relative amplitudes of the various waves are determined primarily by the response of the exciting transducer, which, in these studies, is a broadband 5-MHz unit.

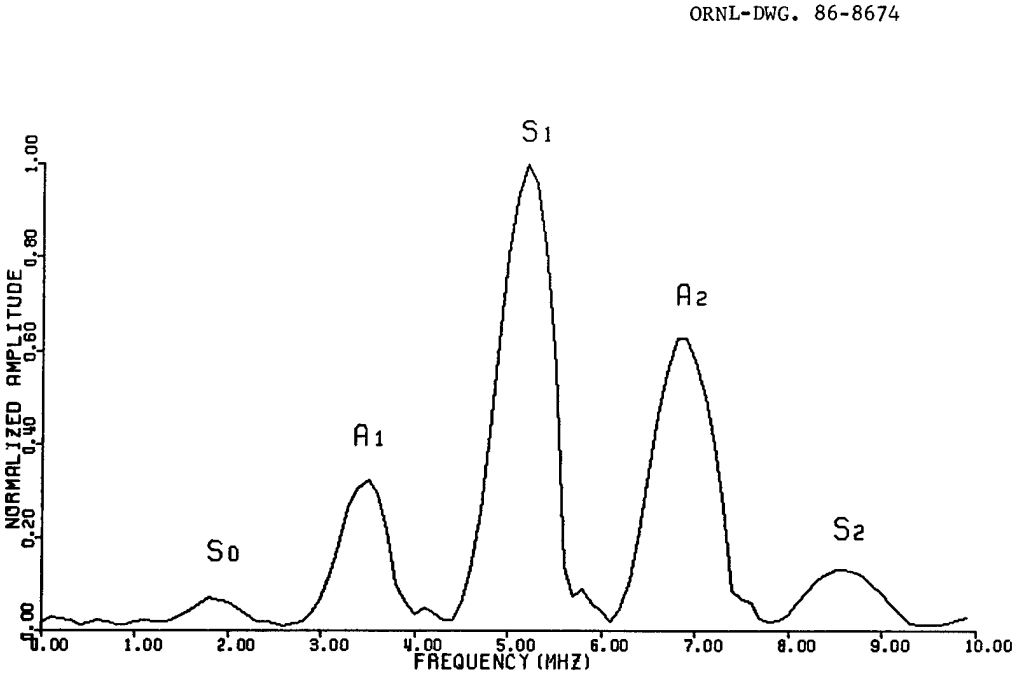

Fig. 23. Spectrum of Lamb wave modes in an alumina coupon.

A pure-mode response can be obtained by using single-frequency excitation of an appropriate transducer. Alternatively, one can use a relatively narrow-band transducer and select a normalized velocity (incident angle) such that only one mode exists within the passband of the transducer. Figure 24 shows the excitation of a single mode, the lowest-order symmetric mode, in an alumina coupon by a 2.25-MHz transducer using pulse excitation.

ORNL-DWG. 86-8675

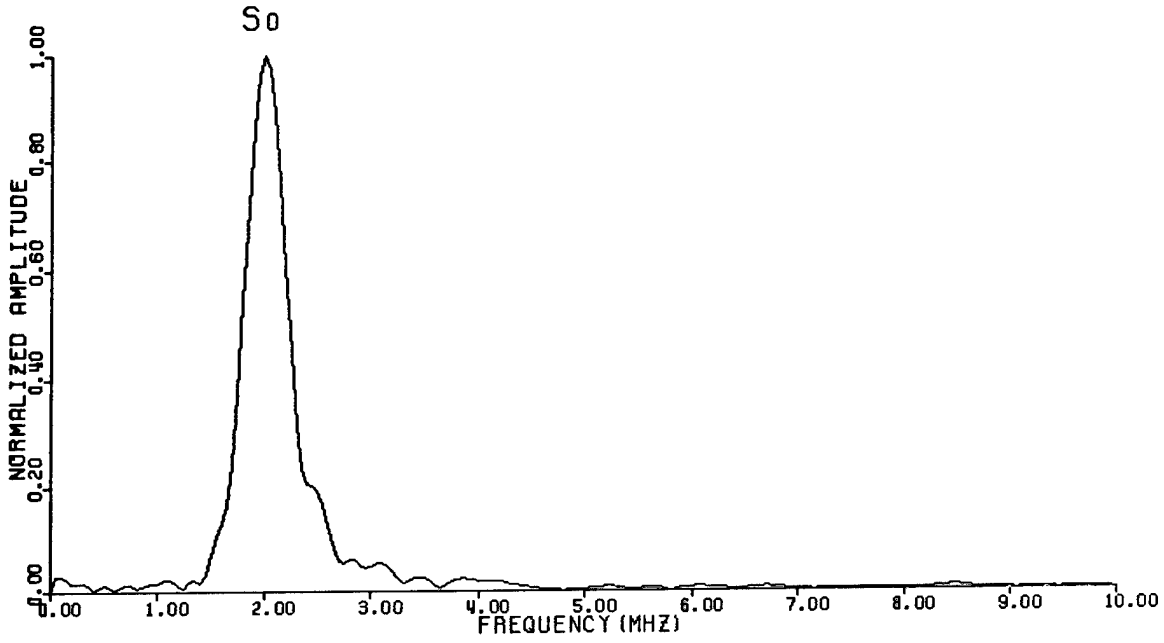

Fig. 24. Excitation of a single Lamb mode in an alumina coupon.

In order to test the effectiveness of using Lamb waves to interrogate the butt-braze joint in alumina flexure-strength specimens, the specially fabricated sample shown in Fig. 25 was made. A piece of tantalum foil at each end of the joint provides the proper separation of the ceramic halves during melting of the braze. A third piece of foil was placed in the center of this particular specimen to prevent bonding in that region and to simulate a nonbond of known dimensions. The brazing filler metal was one of several under development at Oak Ridge National Laboratory that will wet oxide ceramics directly with no pretreatment of the ceramic surface.

YP2042

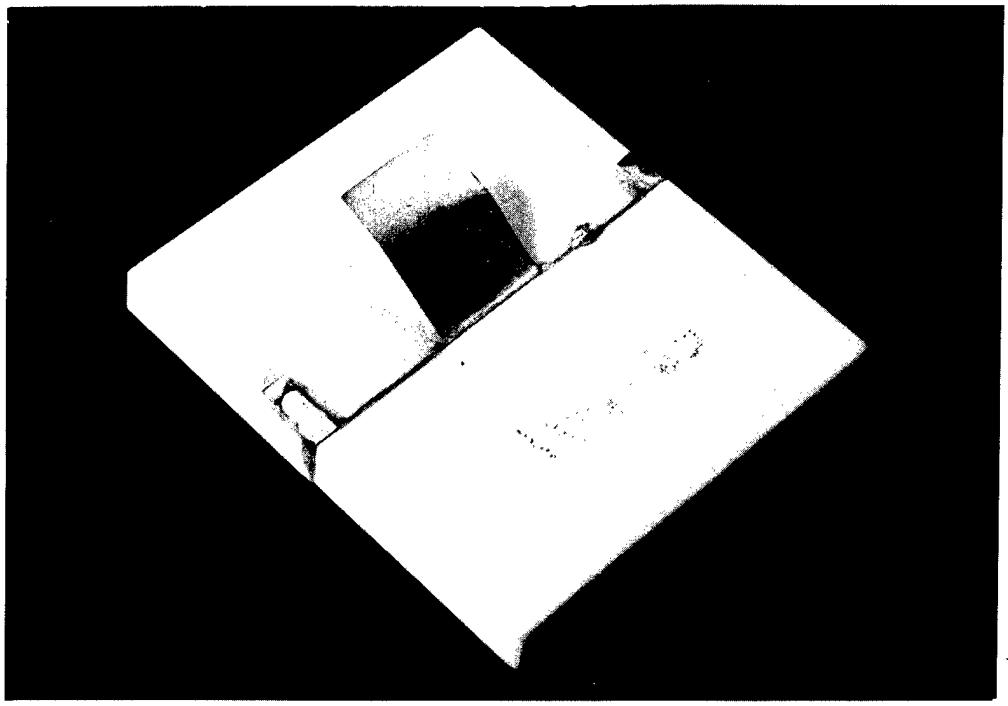

Fig. 25. Flexure-strength specimen containing a simulated nonbond.

The standard was first examined by conventional angle-beam through-transmission techniques using 25-MHz transducers. The joint was scanned in an *x-y* pattern using an index of 100 μm. As expected, the central nonbond was easily detected using both flat and focused transducers. For the latter, the sensitivity varied from top to bottom of the interface because of variations in the beam profile with depth. In both cases, however, numerous indications were generated at the top and bottom of the interface by a slight vertical misalignment of the ceramic coupons. This particular approach is sensitive to misalignment and is a disadvantage of angle-beam testing of butt joints.

We next examined the standard using Lamb waves. Two transducers were used with the transmitter and receiver located on opposite sides of the interface. Figure 26 shows the transducer configuration. The transmitter was driven with a tone burst to ensure excitation of a single Lamb mode.

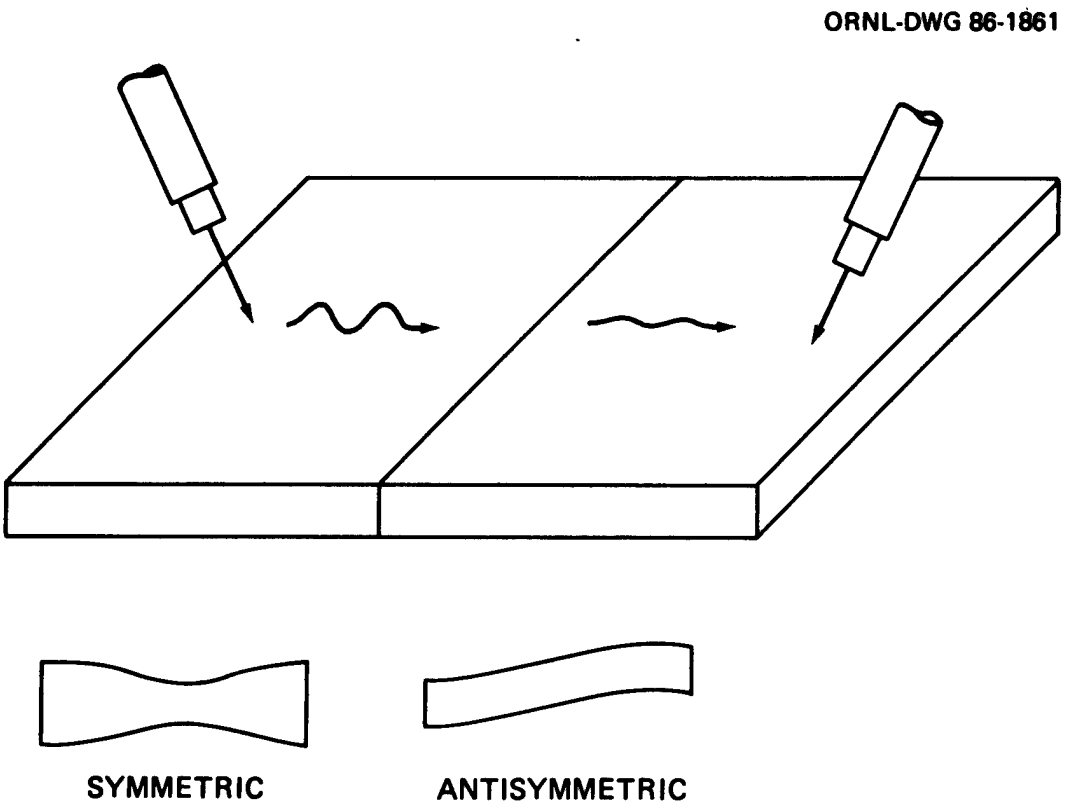

Fig. 26. Transducer configuration for excitation and detection of Lamb waves in the butt-brazed alumina coupon illustrated in Fig. 25.

As expected, virtually no change in transmission amplitude was detected when the transducers were translated perpendicularly to the joint. Nevertheless, an *x-y* scan (parallel and perpendicular to the interface) was made. The results are shown in Fig. 27, where the height of the surface represents the Lamb wave transmission amplitude. The central nonbond corresponds to the large dip in the surface. Obviously, a single scan parallel to the interface would have sufficed, so this test can be performed very rapidly.

A second butt-braze specimen was also available; it was a standard flexure bar consisting of titanium-coated PSZ coupons brazed with a commercial Ag-Cu-Sn filler metal. Only the two end pieces of tantalum foil were present in this sample. It was first tested by conventional angle-beam techniques with no indications detected other than the usual ones attributable to vertical misalignment of the ceramic plates. In particular, no regions of unbonding were found.

YP2039

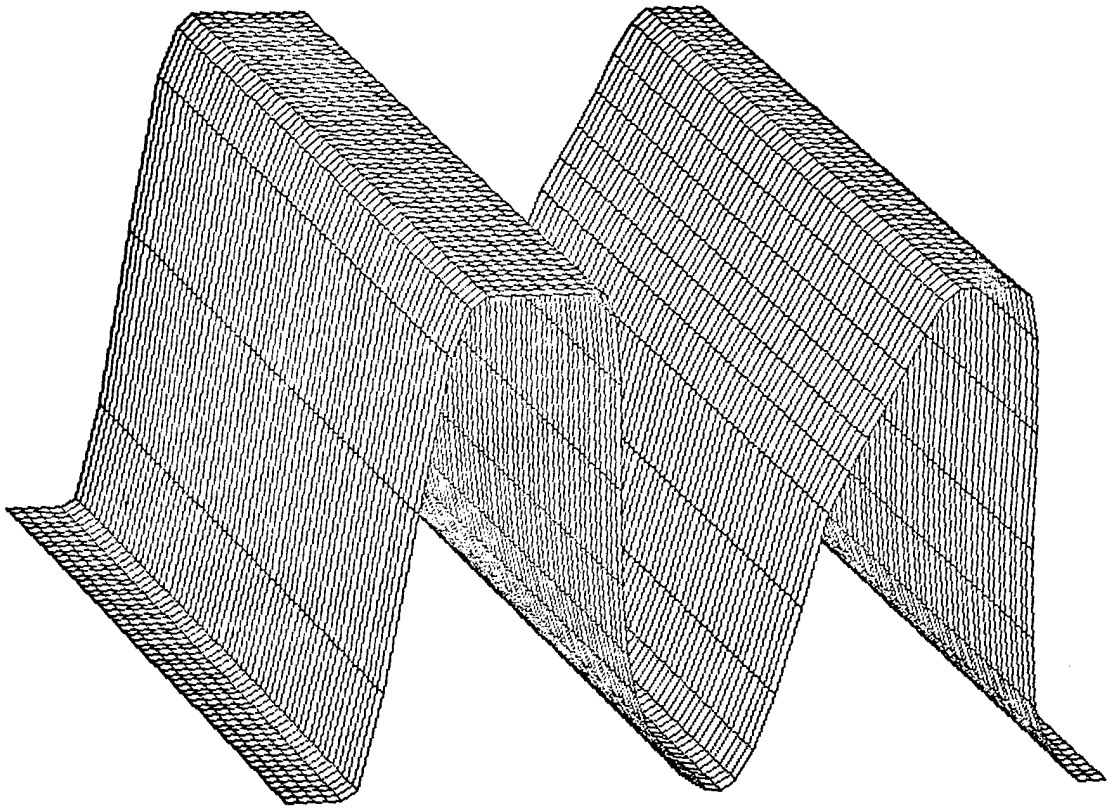

Fig. 27. Lamb wave transmission through the bond of the alumina flexure-strength specimen illustrated in Fig. 25, showing detection of the simulated nonbond.

Figure 28 shows the results obtained with Lamb waves on that second specimen. There is a small region near the center of the braze joint where the Lamb wave transmission dips noticeably. We then switched to a pulse-echo mode; that is, we monitored the amplitude of the Lamb waves reflected by the interface using first one and then the other transducer as a transmitter. In each case, an enhanced reflection was found at the location of the dip in Fig. 28. This eliminates problems in the ceramic (e.g., cracking) away from the interface as the source of the anomaly and establishes that some variation in the region of the interface engendered the signal.

Radiographic examination of the specimen revealed no detectable flaws in the interface.

ORNL-DWG 86-13162

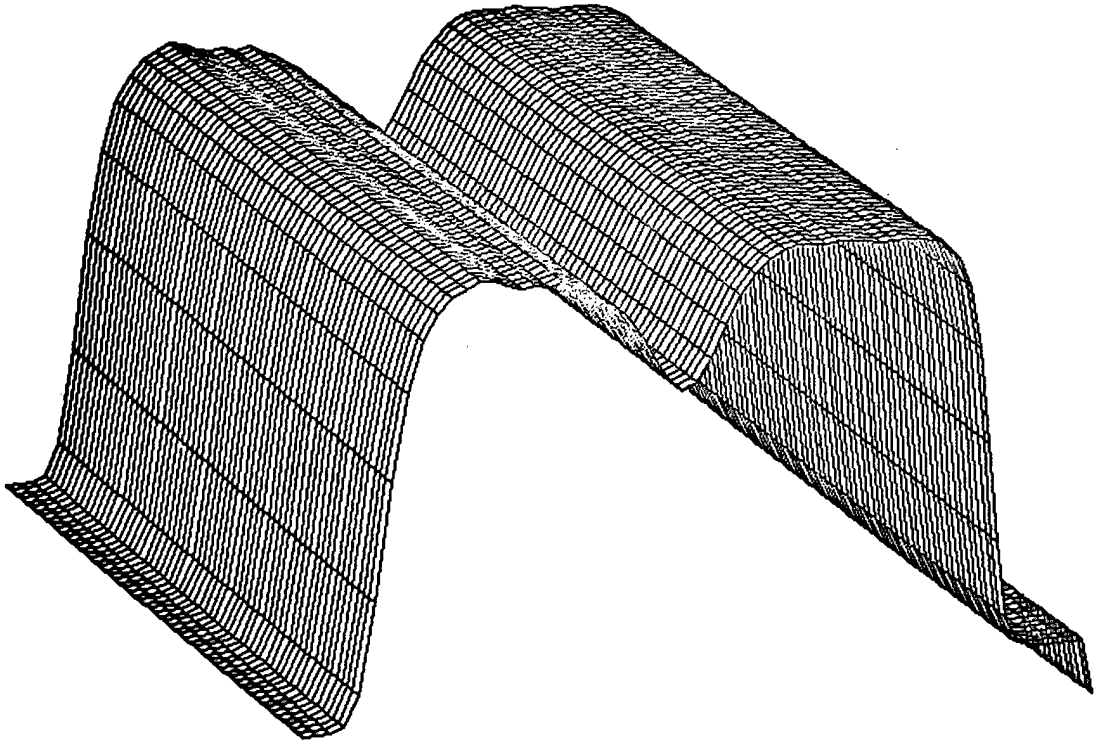

Fig. 28. Lamb wave transmission through the bond of another PSZ flexure-strength specimen having a simulated nonbond, showing a small indication near the center of the bond.

These results indicate that Lamb waves are sensitive to some characteristics of the braze joint that conventional nondestructive test techniques do not detect. The specimen will be cut into flexure bars and subjected to bend tests to try to develop a correlation between the inspection results and the strength of the bond.

SUMMARY AND CONCLUSIONS

The small critical flaw size in conventional monolithic structural ceramics has placed severe burdens on the development of ultrasonic NDE techniques for ensuring the integrity of parts fabricated of these materials. Since the detectability of a given flaw increases as the wavelength of the interrogating radiation decreases (at least until the wavelength becomes comparable to the flaw size), frequencies of at least 50 MHz are required to detect critical flaws in many ceramics. In addition, unlike structural metals, the interrogating ultrasonic radiation

must be focused in order to ensure that a sufficiently large fraction of the incident radiation is intercepted by the flaw. The necessity of introducing focused radiation through the surface of the ceramic part (mandated by the desire to have rapid scanning capability) leads to severe spherical aberration of the ultrasonic beam within the part and limits the depth to which critical flaws can be detected to a few millimeters. Within these constraints, however, we have had considerable success in detecting flaws in the critical size range.

Since a common flaw type in ceramics is a quasi-spherical void or inclusion, a model was discussed for the scattering of ultrasonic waves from spheres. This model was applied to scattering from natural flaws in partially stabilized zirconia, and a flaw diameter of about 25 μm was inferred.

Since the attenuation behavior of structural ceramics for ultrasonic waves is critical to determining the minimum detectable flaw size, a technique was developed that permits a material transfer curve, or attenuation versus frequency response, to be determined for any ceramic. This process corrects for all known material-independent losses, such as diffraction (beam spread), acoustic impedance mismatches at the surfaces of the part and at internal interfaces, and frequency-dependent coupling losses between the transducer and the surface of the part. The transfer curve is highly sensitive to changes in the microstructure of the ceramic, and examples of the differences in TZP and PSZ ceramics were given.

Since current heat engine designs contain components consisting of a ceramic material clad on a metallic substrate to achieve both high-temperature tolerance and toughness, additional evaluation techniques were required for assurance of the quality of a ceramic-metal bond. The braze layer in such a bond is typically of the order of 60 μm thick, and, if nonbonding occurs, the tester needs to determine which face of this layer is nonbonded. For high-frequency ceramics, this condition could be determined by interrogating the bond with frequencies sufficiently high (≈100 MHz) to resolve the layer thickness. Examples were given of the detection of 100-μm-diam pores in the braze layer using this approach. When the ceramic host would not support ultrasonic waves of such a high

frequency, however, advanced signal processing techniques had to be developed to recover the desired information. An example was given of the identification of the correct interface in a braze joint in PSZ.

Although no specimens were available for study that contained manufactured flaws of known size in the bond layer of a ceramic-to-metal joint, a sample containing such flaws at the interface between a P-leg and an N-leg of a silicon-germanium specimen was obtained. The detection of a 125-μm flaw was demonstrated, and the signal-to-noise ratio for this flaw indicates that considerably smaller flaws could be detected reliably.

In testing joints between ceramic coupons, it is often not possible to introduce the ultrasound at normal incidence to the bond because of specimen geometry. In such cases, angle-beam testing techniques can be used, but it is difficult to maintain transducer focus across the full width of the interface. In addition, angle-beam testing was found to be unduly sensitive to slight vertical misalignment of the two plates being joined. For these configurations, a second approach, one using plate or Lamb waves, was studied. Two transducers were used: one launches a Lamb wave in either plate of the specimen, and the second receives the wave in the other plate after propagation through the joint. The amplitude of the received wave is an indicator of the condition of the bond in the region between the transducers.

Dispersion curves for Lamb waves in alumina coupons were calculated, and a system was assembled for evaluation of the bond by these waves. The system was shown to detect a simulated nonbond easily, and inspection of a second sample by this technique revealed an indication in the bond area that was not detected by angle-beam testing.

While bonds between ceramic components and between ceramic and metallic parts present a number of difficult problems to the researcher, considerable progress has been made in developing techniques that will allow the integrity of these bonds to be assured nondestructively. Many problems remain, however. Perhaps the most common criticism directed at ceramic inspection is that it is slow in comparison with inspection of metals. Rarely is it noted, however, that most ceramic inspection systems do not approach the state of the art in data acquisition rates. This is understandable, since technique development is of more importance at the

present time in ceramic evaluation than it is for metals, where the techniques have a long history of development. Inspection rates will undoubtedly increase for ceramic evaluation as the approaches become established.

A more fundamental limitation in ceramic or ceramic-joint evaluation is related to the requirement for focused radiation. The severe aberrations introduced into the beam by propagation through the sample surface limit the depth to which effective focus can be maintained. This depth can be increased somewhat by increasing transducer frequency and focal length, but the relationship does not appear to favor this approach. Some form of this limitation will likely persist in the foreseeable future.

The techniques presented here do not exhaust the potential tools for ceramic-joint evaluation by a wide margin. For example, some form of direct interface wave (i.e., a wave that propagates in the bond material but not in the ceramic) may possibly yield information about the strength of the bond itself. This result would indeed be valuable, since there is currently no known correlation between bond strength and measurable acoustic properties.

ACKNOWLEDGMENTS

The authors thank A. J. Moorhead and M. L. Santella for the design and fabrication of the ceramic-cap piston specimens and the flexure-strength samples used in this study. The shear specimens were kindly provided by J. P. Hammond. The authors gratefully acknowledge helpful discussions of ceramic flaw types and sizes with T. N. Tiegs and P. F. Becher. Thanks are also due to J. L. Bishop for preparing the draft of this report, to O. A. Nelson for editing it, and to A. R. McDonald for final preparation of the report.

REFERENCES

1. C. F. Ying and R. Truell, "Scattering of a Plane Longitudinal Wave by a Spherical Obstacle in an Isotropically Elastic Solid," *J. Appl. Phys.* **27**, 1086 (1956).

2. W. A. Simpson, Jr., L. Adler, K. V. Cook, and R. W. McClung, *Ultrasonic Flaw Characterization Techniques for Stainless Steel Welds*, ORNL-6175, January 1986.

3. M. L. Santella, J. P. Hammond, S. A. David, and W. A. Simpson, "Zirconia to Cast Iron Brazing for Uncooled Diesel Engines," pp. 235–41 in *Proceedings of the Twenty-Third Automotive Technology Development Contractors' Coordination Meeting, P-165, Dearborn, Michigan, Oct. 21–24, 1985*, Society of Automotive Engineers, Warrendale, Pa., 1985.

4. W. A. Simpson, Jr., "Time-Domain Deconvolution: A New Technique to Improve Resolution for Ultrasonic Flaw Characterization in Stainless Steel Welds," *Mat. Eval.* 44(8), 998–1003 (1986).

5. S. I. Rohklin, "Interface Properties Characterization by Elastic Guided Waves," presented at the 1985 Review of Progress in Quantitative NDE, Williamsburg, VA., June 23–28, 1985.

ORNL-6350

INTERNAL DISTRIBUTION

1–2. Central Research Library
3. Document Reference Section
4–5. Laboratory Records Department
6. Laboratory Records, ORNL RC
7. ORNL Patent Section
8. P. F. Becher
9. R. A. Bradley
10. C. R. Brinkman
11. R. A. Buhl
12. V. R. Bullington
13. A. J. Caputo
14. R. S. Carlsmith
15. J. A. Carpenter, Jr.
16. K. V. Cook
17. D. F. Craig
18. S. A. David
19. C. K. DuBose
20. R. S. Graves
21. C. Hsueh
22. D. R. Johnson
23. R. R. Judkins
24. J. F. Martin
25–29. R. W. McClung
30. A. J. Moorhead
31. R. K. Nanstad
32. D. F. Pedraza
33. M. L. Santella
34. A. C. Schaffhauser
35–39. W. A. Simpson, Jr.
40. G. M. Slaughter
41. J. H. Smith
42. J. O. Stiegler
43–45. P. T. Thornton
46. J. R. Weir
47. R. O. Williams
48. A. Zucker
49. G. Y. Chin (Consultant)
50. H. E. Cook (Consultant)
51. F. F. Lange (Consultant)
52. T. E. Mitchell (Consultant)
53. W. D. Nix (Consultant)
54. J. C. Williams (Consultant)

EXTERNAL DISTRIBUTION

55. Donald F. Adams
Composite Materials Research Group
Mechanical Engineering Department
University of Wyoming
Laramie, WY 82071

56. Jane W. Adams
Corning Glass Works
SP-DV-21
Corning, NY 14831

57. Donald J. Adrian
Chief Engineer
High Velocity Tool Corporation
2015 Indiana Street
Racine, WI 53405

58. Bruce J. Agle
Metallurgical Engineer
Sundstrand Corporation
Turbomach Division
Advanced Technology Group
4400 Ruffin Road
PO Box 85757
San Diego, CA 92138-5757

59. Richard T. Alpaugh
Department of Energy
Office of Transportation Systems
Forrestal Building CE-151
1000 Independence Avenue
Washington, DC 20585

60. H. Arbabi
Brunel University
Department of Materials
Technology
Uxbridge Middlesex UB8 3PH
United Kingdom

61. James P. Arnold
U.S. Army Belvoir
R&D Center
ATTN: FTRBE-EMP
Fort Belvoir, VA 22060

62. V. S. Avva
North Carolina Agricultural and
Technical State University
Department of Mechanical
Engineering
Greensboro, NC 27411

63. John M. Bailey
Research Consultant
Research Department
Technical Center
Caterpillar Tractor Company
100 NE Adams
Peoria, IL 61629

64. Murray Bailey
NASA Lewis Research Center
21000 Brookpark Road, MS 77-6
Cleveland, OH 44135

65. R. R. Baker
Ceradyne, Inc.
3030-A S. Red Hill Avenue
Santa Ana, CA 92705

66. J. Gary Baldoni
GTE Laboratories, Inc.
40 Sylvan Road
Waltham, MA 02254

67. Ken Baumert
Air Products and Chemicals, Inc.
Box 538
Allentown, PA 18105

68. A. L. Bement, Jr.
Vice President
Technical Resources
TRW, Inc.
23555 Euclid Avenue
Cleveland, OH 44117

69. M. Bentele
Xamag, Inc.
259 Melville Avenue
Fairfield, CT 06430

70. Clifton G. Bergeron
Head, Department of
Ceramic Engineering
University of Illinois
204 Ceramics Building
Urbana, IL 61801

71. William D. Bjorndahl
TRW, Inc.
TRW Energy Development Group
Materials Characterization
and Chemical Analysis Dept.
One Space Park
Building 01, Room 2060
Redondo Beach, CA 90278

72. James A. Black
Vice President
American Matrix, Inc.
118 Sherlake Drive
Knoxville, TN 37922

73. John Blum
Norton Company
High Performance Ceramics
Goddard Road
Northboro, MA 01532-1545

74. Paul N. Blumberg
President
Integral Technologies Inc.
415 E. Plaza Drive
Westmont, IL 60559

75. Wolfgang D. G. Boecker
Sohio Engineered Materials
Company
Niagara Falls R&D Center
PO Box 832
Niagara Falls, NY 14302

76. Tibor Bornemisza
Sundstrand Corporation
Project Engineer
Turbomach Division
Advanced Technology Group
4400 Ruffin Road, PO Box 85757
San Diego, CA 92138-5757

77. Seymour A. Bortz
Manager, Nonmetallic Materials and Composites
Materials and Manufacturing Technology
IIT Research Institute
10 West 35th Street
Chicago, IL 60616

78. H. K. Bowen
Department of Materials Science and Engineering, Room 12-009
Massachusetts Institute of Technology
Cambridge, MA 02139

79. Richard C. Bradt
Chairman, Materials Science and Engineering
University of Washington
Dept. of Materials Science and Engineering
Roberts Hall, FB-10
Seattle, WA 98195

80. Raymond J. Bratton
Manager, Ceramic Science
Westinghouse Electric Corporation
R&D Center
1310 Beulah Road
Pittsburgh, PA 15235

81. Catherine E. Brown
E. I. DuPont de Nemours & Company
Experimental Station
Information Center E302/301
Wilmington, DE 19898

82. J. J. Brown
Virginia Polytechnic Institute and State University
Department of Materials Engineering
Blacksburg, VA 24061

83. W. Bryzik
U.S. Army Tank Automotive Command
R&D Center, Propulsion Systems Division
Warren, MI 48090

84. S. T. Buljan
GTE Laboratories, Inc.
40 Sylvan Road
Waltham, MA 02254

85. John M. Byrne, Jr.
Manager, Business Development
Corporate Development Department
PPG Industries, Inc.
One PPG Place
Pittsburgh, PA 15272

86. Donald J. Campbell
Air Force Wright Aeronautical Laboratory
AFWAL/POX
Wright-Patterson Air Force Base
OH 45433

87. Harry W. Carpenter
Rockwell International
Rocketdyne Division
J39-169-FB39
6633 Canoga Avenue
Canoga Park, CA 91304

88. David Carruthers
Garrett Turbine Engine Company
111 South 34 Street
PO Box 5217
Phoenix, AZ 85010

89. Se-Tak Chang
GTE Laboratories
40 Sylvan Road
Dept. 312
Waltham, MA 02254

90. R. J. Charles, Manager
Ceramics Branch
Physical Chemistry Laboratory
General Electric Company
PO Box 8
Schenectady, NY 12301

91. En-sheng Chen
B&C Engineering Research
13906 Dentwood Drive
Houston, TX 77014

92. Albert A. Chesnes
Director, Heat Engine
Propulsion Division
Office of Transportation Systems
Department of Energy
Forrestal Building CE-151
1000 Independence Avenue
Washington, DC 20585

93. Frank Childs
EG&G, Inc.
Idaho National Engineering
Laboratory
PO Box 1625
Idaho Falls, ID 83415

94. Melvin H. Chiogioji
Director, Office of
Transportation Systems
Department of Energy
Forrestal Building CE-15
1000 Independence Avenue, SW
Washington, DC 20585

95. William J. Chmura
The Torrington Company
Corporate Research
59 Field Street
Torrington, CT 06790

96. Eugene V. Clark
Vice President
Technology Engineering
Turbine Metal Technology, Inc.
7327 Elmo Street
Tujunga, CA 91042-2204

97. William L. Cleary
Associate Division Director
ORI, Inc.
1375 Piccard Drive
Rockville, MD 20850

98. Jack L. Clem
General Manager
Carbon Black Division
Huber Technology Group
J. M. Huber Corporation
PO Box 2831
Borger, TX 79008-2831

99. Philip R. Compton
Energy Systems Office
National Aeronautics and
Space Administration
Code REC-1
Washington, DC 20546

100. Stephen Copley
Professor and Chairman
Materials Science Department
University of Southern
California
Los Angeles, CA 90089-0241

101. John A. Coppola
Manager, Advanced Programs
Structural Ceramics Division
Standard Oil Engineered Materials
Company
PO Box 1054
Niagara Falls, NY 14302

102. William J. Croft
U.S. Army Materials Technology
Laboratory
Arsenal Street
Watertown, MA 02172

103. Gary M. Crosbie
Ford Motor Company
PO Box 2053, Room S-2079
Ceramics Materials Department
Dearborn, MI 48121

104. Floyd W. Crouse, Jr.
Department of Energy
Morgantown Energy Technology
Center
PO Box 880
Morgantown, WV 26505

105. Raymond Cutler
Ceramatec, Inc.
163 W. 1700 South
Salt Lake City, UT 84115

106. David A. Dalman
Research Manager
Central Research
Organic Specialties Lab
Dow Chemical Company
M. E. Pruitt Building
Midland, MI 48640

107. Stephen C. Danforth
Rutgers University
PO Box 909
Piscataway, NJ 08854

108. Stanley J. Dapkunas
Ceramic Division
Institute for Materials Science and Engineering
National Bureau of Standards
Gaithersburg, MD 20899

109. Robert F. Davis
North Carolina State University
Materials Engineering Department
232 Riddick Laboratory
Raleigh, NC 27607

110. Evelyn M. DeLiso
Assistant Research Professor
Center for Ceramics Research
Rutgers University
College of Engineering
PO Box 909
Piscataway, NJ 08854

111. Alan L. Dragoo
Materials Scientist
Inorganic Materials Division
National Bureau of Standards
Center for Materials Science
Gaithersburg, MD 20899

112. Keith F. Dufrane
Battelle Columbus Laboratories
505 King Avenue
Columbus, OH 43201

113. Robert J. Eagan
Manager, Chemistry and Ceramics Department 1840
Sandia National Laboratories
Albuquerque, NM 87185

114. Christopher A. Ebel
Program Manager
High Performance Ceramics
Norton Company
Goddard Road
Northboro, MA 01532

115. J. J. Eberhardt
Director, Energy Conversion and Utilization Technologies Program
Department of Energy
Forrestal Building CE-12
1000 Independence Ave SW
Washington, DC 20585

116. E. E. Ecklund
Office of Transportation Systems
Department of Energy
Forrestal Building CE-151
1000 Independence Avenue
Washington, DC 20585

117. William A. Ellingson
Argonne National Laboratory
9700 South Cass Avenue
Argonne, IL 60439

118. Director, Applied Technology Laboratory
U.S. Army Research and Technology Laboratory (AVSCOM)
ATTN: SAVDL-ATL-ATP
(Mr. Graydon A. Elliott)
Fort Eustis, VA 23604

119. A. Erdely
Chemical Engineer
26 Av. Gare des Eaux-vives
1208 Geneva
Switzerland

120. Charles D. Estes
U.S. Senate
Professional Staff Member
Committee on Appropriations
SD-152 Dirksen Senate Office Building
Washington, DC 20510

121. Anthony G. Evans
University of California
College of Engineering
Santa Barbara, CA 93106

122. Robert C. Evans
Asst. Manager, Vehicular Gas Turbine and Diesel Project Office
NASA Lewis Research Center
21000 Brookpark Road
Cleveland, OH 44135

123. Katherine T. Faber
Assistant Professor of Ceramic Engineering
Ohio State University
2041 College Road
Columbus, OH 43210

124. John Facey
National Aeronautics and Space Administration
Energy Systems Office
Washington, DC 20546

125. John W. Fairbanks
Office of Transportation Systems
Department of Energy
Forrestal Building CE-151
Washington, DC 20585

126. Larry Farrell
Babcock and Wilcox
PO Box 1260
Lynchburg, VA 24505

127. M. K. Ferber
University of Illinois
105 S. Goodwin Avenue
203 Ceramic Building
Urbana, IL 61801

128. H. W. Foglesong
Dow Corning Corporation
3901 S. Saginaw Road
Midland, MI 48640

129. Thomas F. Foltz
Manager, Product Applications
Avco
Special Materials Division
Two Industrial Avenue
Lowell, MA 01851

130. Robert G. Frank
Manager, Non-Metallic Materials
General Electric Company
One Neumann Way
Mail Drop M-87
PO Box 156301
Cincinnati, OH 45215-6301

131. Frank Gac
Los Alamos National Laboratory
PO Box 1663
MSP6 MS G-770
Los Alamos, NM 87545

132. George E. Gazza
U.S. Army Materials Technology Laboratory
Ceramics Research Division
Arsenal Street
Watertown, MA 02171

133. Charles M. Gilmore
Department of Civil, Mechanical, and Environmental Engineering
The George Washington University
Washington, DC 20052

134. Paul Glance
Director, R&D
Concept Analysis Corporation
9145 General Court
Plymouth, MI 48170

135. Fred M. Glaser
Department of Energy
Office of Fossil Energy, FE-14
Washington DC 20545

136. Joseph W. Glatz
Naval Air Propulsion Test Center
Science and Technology Group
Systems Technology Division
Box 7176, PE 34
Trenton, NJ 08628

137. Stephen T. Gonczy
Allied Signal Research Center
Materials Science Department
50 UOP Plaza
Des Plaines, IL 60016-6187

138. Robert J. Gottschall
Office of Material Sciences
Department of Energy
ER-131 GTN
Washington, DC 20545

139. Kenneth Green
Senior Development Engineer
Coors Porcelain Company
Golden, CO 80401

140. Michael Greenfield
National Aeronautics and
Space Administration
Energy Systems Office
Washington, DC 20546

141. Lance E. Groseclose
General Motors Corporation
Allison Gas Turbine Division
PO Box 420
Indianapolis, IN 46206-0420

142. T. D. Gulden
Manager, Ceramics and
Chemistry
GA Technologies, Inc.
PO Box 81608
San Diego, CA 92138

143. M. D. Gurney
NIPER
PO Box 2128
Bartlesville, OK 74005

144. J. J. Habeeb
Senior Chemist
Research Division
Esso Petroleum Canada
PO Box 3022
Sarina, Ontario
Canada N7T 7M1

145. H. T. Hahn
Pennsylvania State
University
ESM Department
227 Hammond Building
University Park, PA 16802

146. Nabil S. Hakim
Staff Research Engineer,
Engineering R&D
General Motors Corporation
Detroit Diesel Allison
Division
36880 Ecorse Road
Romulus, MI 48174

147. John W. Halloran
Ceramic Process Systems
128 Spring Street
Lexington, MA 02173

148. R. A. Harmon
25 Schalren Drive
Latham, NY 12110

149. Stephen D. Hartline
Norton Company
High Performance Ceramics
Goddard Road
Northboro, MA 01532

150. Willard E. Hauth
Section Manager, Composite
Development Ceramics Program
Dow Corning Corporation
Midland, MI 48640

151. Norman L. Hecht
University of Dayton Research Institute
300 College Park
Dayton, OH 45469-0001

152. S. S. Hecker
Deputy Division Leader
Material Science and Technology Division, G-756
Los Alamos National Laboratory
PO Box 1663
Los Alamos, NM 87545

153. Peter W. Heitman
General Motors Corporation
Allison Gas Turbine Operations
PO Box 420, W-5
Indianapolis, IN 46206-0420

154. Richard L. Helferich
The Duriron Company, Inc.
PO Box 1145
Dayton, OH 45401

155. H. E. Helms
General Motors Corporation
Allison Gas Turbine Operations
PO Box 420
Indianapolis, IN 46206-0420

156. Thomas L. Henson
Director of Research and Engineering
Chemical & Metallurgical Division
GTE Products Corporation
Hawes Street
Towanda, PA 18848-0504

157. Thomas P. Herbell
NASA Lewis Research Center
21000 Brookpark Road
MS 105-1
Cleveland, OH 44135

158. Ben Heshmatpour
Thermo Electron Corporation
101 First Avenue
Waltham, MA 02154

159. Hendrik Heystek
Bureau of Mines
Tuscaloosa Research Center
PO Box L
University, AL 35486

160. Robert V. Hillery
Manager, Coating Materials and Processes
General Electric Company
Cincinnati, OH 45215

161. Jonathan W. Hinton
Vice President and General Manager
Structural Ceramics Division
Standard Oil Engineered Materials
PO Box 1054
Niagara Falls, NY 14302

162. James C. Holzwarth
General Motors Research Laboratories
2629 Saturn Drive Lake
Orion, MI 48035

163. Stephen M. Hsu
Chief, Ceramics Division
Institute for Materials Science & Engineering
National Bureau of Standards
Gaithersburg, MD 20899

164. Harold A. Huckins, President
Princeton Advanced Technology, Inc.
56 Finley Road
Princeton, NJ 08540

165. Joseph E. Hunter, Jr.
General Motors Corporation
Research Labs, Metallurgy Department
12 Mile and Mound Roads
Warren, MI 48090-9055

166. Louis C. Ianniello
Director, Office of Materials Sciences
Department of Energy
ER-13 GTN
Washington, DC 20545

167. Robert H. Insley
Champion Spark Plug Company
Ceramic Division
20000 Conner Avenue
Detroit, MI 48234

168. Curt A. Johnson
General Electric Company
Physical Chemistry Laboratory
PO Box 8
Schenectady, NY 12301

169. Douglas C. Johnson
Technology Development Manager
Sundstrand Corporation
Turbomach Division
4400 Ruffin Road, PO Box 85757
San Diego, CA 92138-5757

170. Larry Johnson, Director
Center for Transportation Research
Argonne National Laboratory
9700 S. Cass Avenue, Building 362
Argonne, IL 60439

171. R. A. Johnson
General Motors Corporation
Allison Gas Turbine Division
PO Box 420
Indianapolis, IN 46206-0420

172. L. A. Joo
Associate Director of Research
Great Lakes Research Corporation
PO Box 1031
Elizabethton, TN 37643

173. A. David Joseph
Vice President, R&D Engineering
Sealed Power Corporation
100 Terrace Plaza
Muskegon, MI 49443

174. Roy Kamo, President
Adiabatics, Inc.
630 S. Mapleton
Columbus, IN 47201

175. Allan Katz
Air Force Wright
Aeronautical Laboratory
Materials Laboratory, AFWAL/MLLM
Metals and Ceramics Division
Wright-Patterson Air Force Base
OH 45433

176. R. N. Katz
Chief, Ceramics Research
Division
U.S. Army Materials
Technology Laboratory
Arsenal Street
Watertown, MA 02172

177. Frank N. Kelley
Director
Institute of Polymer Science
The University of Akron
Akron, OH 44325

178. P. Victor Kelsey
Ceramics Technical Leader
Materials Science Division
Aluminum Company of America
Alcoa Technical Center B
Alcoa Center, PA 15061

179. Frederick L. Kennard, III
Supervisor, Ceramic Research
General Motors Corporation
AC Spark Plug Division,
Dept. 32-24
1300 N. Dort Highway
Flint, MI 48556

180. J. R. Kidwell
AGT101 Assistant Project
Engineer
Garrett Turbine Engine Company
111 S. 34th Street
PO Box 5217
Phoenix, AZ 85010

181. Max Klein
Senior Scientist
Thermodynamics
Gas Research Institute
8600 West Bryn Mawr Avenue
Chicago, IL 60631

182. C. E. Knapp
Norton Company
8001 Daly Street
Niagara Falls, Ontario
Canada

183. A. S. Kobayashi
University of Washington
Dept. of Mechanical Engineering
MS FU10
Seattle, WA 98195

184. James F. Kolbe
Group Vice President
Product Development and
Engineering Services Group
Sealed Power Corporation
100 Terrace Plaza
Muskegon, MI 49443

185. David M. Kotchick
AiResearch Manufacturing Company
2525 W. 190th Street
Torrance, CA 90509

186. Bruce Kramer
George Washington University
Aerodynamic Center, Room T715
Washington, DC 20052

187. Saunders B. Kramer
Manager, AGT Program
Office of Transportation Systems
Department of Energy
Forrestal Building CE-151
1000 Independence Avenue
Washington, DC 20585

188. D. M. Kreiner
AGT101 Project Manager
Garrett Turbine Engine Company
111 S. 34th Street, PO Box 5217
Phoenix, AZ 85010

189. Pieter Krijgsman
Ceramic Design Int. Hold., Ltd.
PO Box 68
8050 AB Hattem
The Netherlands

190. W. J. Lackey
Georgia Tech Research Institute
Energy and Materials Sciences
Laboratory
Georgia Institute of Technology
Atlanta, GA 30332

191. Everett A. Lake
Air Force Wright
Aeronautical Laboratory
AFWAL/POOS
Wright-Patterson Air Force Base
OH 45433

192. James Lankford
Department of Materials
Sciences
Southwest Research Institute
6220 Culebra Road
PO Drawer 28510
San Antonio, TX 78284

193. John G. Lanning
Corning Glass Works
Advanced Engine Components
HP-BB-2
Corning, NY 14830

194. David C. Larsen
Corning Glass Works
Materials Research
Department
Sullivan Park, FR-51
Corning, NY 14831

195. Patrick Lauzon
Ontario Research Foundation
Glass and Ceramics Centre
Materials Division
Sheridan Park Research
Community
Mississauga, Ontario
Canada L5K 183

196. Harry A. Lawler
Senior Product Specialist
Structural Ceramics Division
Standard Oil Engineered
Materials Company
PO Box 1054, Bldg. 91-2
Niagara Falls, NY 14302

197. Alan Lawley
Drexel University
Materials Engineering
Philadelphia, PA 19104

198. Daniel Lee
Temescon
2850 7th Street
Berkeley, CA 94710

199. June-Gunn Lee
Head, Refractory Materials
Korea Advanced Institute of Science and Technology
PO Box 131, Dong Dae Mun
Seoul
Korea

200. E. M. Lenoe
Office of Naval Research
Air Force Office of Scientific Research
Liaison Office, Far East
APO San Francisco, CA 96503-0110

201. Stanley R. Levine
NASA Lewis Research Center
21000 Brookpark Road
Cleveland, OH 44135

202. David Lewis
Naval Research Laboratory
Code 6360, Materials Science and Technology Division
4555 Overlook Avenue, SW
Washington, DC 20375

203. Winston W. Liang
Director of Program Development
Amercom, Inc.
8948 Fullbright Avenue
Chatsworth, CA 91311

204. Bill Long
Babcock and Wilcox
PO Box 1260
Lynchburg, VA 24505

205. L. A. Lott
EG&G, Inc.
Idaho National Engineering Laboratory
PO Box 1625
Idaho Falls, ID 83415

206. Bryan K. Luftglass
Staff Consultant
Chem Systems, Inc.
303 S. Broadway
Tarrytown, NY 10591

207. Michael J. Lynch
General Electric Company
Medical Systems Group
PO Box 414, 7B-36
Milwaukee, WI 53201

208. Vincent L. Magnotta
Senior Principal Development Engineer
Technical Diversification
R&D Dept.
Air Products and Chemicals, Inc.
PO Box 538
Allentown, PA 18105

209. Tai-il Mah
Technical Manager, Ceramics and Composites Research
Universal Energy Systems
4401 Dayton-Xenia Road
Dayton, OH 45432

210. L. Manes
Material Scientist
Division of Prospective Studies and Knowledge Transfer
Commission of the European Communities
Joint Research Centre
Ispra Establishment
1-21020 Ispra (Varese)
Italy

211. Gerald R. Martin
Manager, Technology
Fleetguard, Inc.
Cookeville, TN 38501

212. John Mason
Vice President, Engineering
The Garrett Corporation
9851 Sepulveda Boulevard
PO Box 92248
Los Angeles, CA 90009

213. J. McCauley
U.S. Army Materials Technology Laboratory
DRXMR-MC
Arsenal Street
Watertown, MA 02172

214. Robert R. McDonald
President
Boride Products
2879 Aero Park Drive
Traverse City, MI 49684

215. William J. McDonough
Department of Energy
Office of Transportation Systems
Forrestal Building CE-151
1000 Independence Avenue
Washington, DC 20585

216. Thomas D. McGee
Iowa State University
Department of Materials Science and Engineering
Ames, IA 50011

217. Malcolm G. McLaren
Head, Department of Ceramics
Rutgers University
Busch Campus
Bowser Road, Box 909
Piscataway, NJ 08854

218. Arthur F. McLean
Manager, Ceramics Materials Department
Ford Motor Company
20000 Rotunda Drive
Dearborn, MI 48121

219. Brian L. Mehosky
Development Engineer, R&D
Standard Oil Engineered Materials
4440 Warrensville Center Rd.
Cleveland, OH 44128

220. P. K. Mehrotra
Kennametal, Inc.
PO Box 639
Greensburg, PA 15601

221. Joseph J. Meindl
Reynolds International, Inc.
PO Box 27002
6603 W. Broad St.
Richmond, VA 23261

222. D. Messier
U.S. Army Materials Technology Laboratory
DRXMR-MC
Arsenal Street
Watertown, MA 02172

223. Arthur G. Metcalfe
Director
Research Department
Solar Turbines, Inc.
2200 Pacific Highway
PO Box 80966
San Diego, CA 92138

224. Thomas N. Meyer
Senior Technical Specialist
Alumina, Chemicals and Ceramics Division
Aluminum Company of America
Alcoa Technical Center
Alcoa Center, PA 15069

225. W. Miloscia
Standard Oil Engineered Materials
Research and Development
4440 Warrensville Center Rd.
Cleveland, OH 44128

226. Bill Moehle
Ethyl Corporation
451 Florida Blvd.
Ethyl Tower
Baton Rouge, LA 70801

227. Helen Moeller
Babcock and Wilcox
PO Box 11165
Lynchburg, VA 24506

228. Thomas Morel
Vice President
Integral Technologies Inc.
415 E. Plaza Drive
Westmont, IL 60559

229. Frederick E. Moreno, President
Turbo Energy Systems, Inc.
350 Second Street, Suite 5
Los Altos, CA 94022

230. Peter E. D. Morgan
Member Technical Staff
Structural Ceramics
Rockwell International
Science Center
1049 Camino Dos Rios
PO Box 1085
Thousand Oaks, CA 91360

231. Solomon Musikant
General Electric Company
Space Systems Division
PO Box 8555, Mail Stop U-1219
Philadelphia, PA 19101

232. Pero Nannelli
Pennwalt Corporation
900 First Avenue, PO Box C
King of Prussia, PA 19406-0018

233. Robert M. Neilson, Jr.
EG&G Idaho, Inc.
Materials Research
PO Box 1625
Idaho Falls, ID 83415

234. Dale E. Niesz
Manager, Materials
Department
Battelle Columbus
Laboratories
505 King Avenue
Columbus, OH 43201

235. Dick Nixdorf
Vice President
American Matrix, Inc.
118 Sherlake Drive
Knoxville, TN 37922

236. Norton Company
HPC Library/D. M. Jacques
Goddard Road
Northboro, MA 01532-1545

237. W. Richard Ott
New York State College of
Ceramics
Alfred University
Alfred, NY 14802

238. Muktesh Paliwal
GTE Products Corporation
Hawes Street
Towanda, PA 18848

239. Hayne Palmour III
North Carolina State
University
Engineering Research
Services Division
2158 Burlington Engineering
Laboratories
PO Box 5995
Raleigh, NC 27607

240. Joseph N. Panzarino
Norton Company
Director, R&D, High Performance
Ceramics
Goddard Road
Northboro, MA 01532-1545

241. Pellegrino Papa
Manager, Technical and Business
Development
Corning Technical Products
Division
Corning, NY 14831

242. James G. Paschal
Chemical Sales, Regional Manager
Reynolds Metals Company
PO Box 76154
Atlanta, GA 30358

243. Arvid E. Pasto
Member of Technical Staff
Precision Materials Technology
GTE Laboratories, Inc.
40 Sylvan Road
Waltham, MA 02254

244. James W. Patten
Director, Materials Engineering
Cummins Engine Company, Inc.
Box 3005, Mail Code 50183
Columbus, IN 47201

245. Robert A. Penty
Development Engineer
Manufacturing Technology Dept.
Apparatus Division
Eastman Kodak Company
901 Elmgrove Road
Rochester, NY 14650

246. Gary R. Peterson
U.S. Department of Energy
Idaho Operations Office
785 DOE Place
Idaho Falls, ID 83402

247. Dan Petrak
Babcock and Wilcox
PO Box 1260
Lynchburg, VA 24505

248. R. Byron Pipes
University of Delaware
Center for Composite
Materials
2001 Spencer Laboratory
Newark, DE 19716

249. Robert C. Pohanka
Office of Naval Research
800 N. Quincy Street
Code 431
Arlington, VA 22217

250. Stephen C. Pred
Product Manager
ICD Group, Inc.
641 Lexington Avenue
New York, NY 10022

251. Karl M. Prewo
United Technologies Corp.
Research Center
Silver Lane, MS 24
East Hartford, CT 06108

252. Hubert B. Probst
Chief Scientist, Materials
Div., MS
NASA Lewis Research Center
21000 Brookpark Road
Cleveland, OH 44135

253. Carr Lane Quackenbush
Norton Company
High Performance Ceramics
Goddard Road
Northboro, MA 01532-1545

254. George Quinn
U.S. Army Materials
Technology Laboratory
Arsenal Street
Watertown, MA 02172

255. Dennis T. Quinto
Kennametal, Inc.
Phillip M. McKenna
Laboratory
PO Box 639
Greensburg, PA 15601

256. S. Venkat Raman
Manager, New Technology
Marketing
Contract Research Dept.
Air Products and Chemicals, Inc.
PO Box 538
Allentown, PA 18105

257. Dennis Readey
Department Chairman
Ceramic Engineering
Ohio State University
2041 College Road
Columbus, OH 43210

258. Robert R. Reeber
U.S. Army Research Office
PO Box 12211
Research Triangle Park, NC 27709

259. K. L. Reifsnider
Virginia Polytechnic Institute
and State University
Department of Engineering
Science and Mechanics
Blacksburg, VA 24061

260. Paul Rempes
Champion Spark Plug Company
Ceramic Division
20000 Conner Avenue
Detroit, MI 48234

261. T. M. Resetar
U.S. Army Materials
Technology Laboratory
DRXMR-MC
Arsenal Street
Watertown, MA 02472

262. K. T. Rhee
Rutgers University
College of Engineering
PO Box 909
Piscataway, NJ 08854

263. Roy W. Rice
W. R. Grace and Company
7379 Route 32
Columbus, MD 21044

264. David W. Richerson
Ceramatec, Inc.
163 West 1700 South
Salt Lake City, UT 84115

265. Paul Rieth
Ferro Corporation
661 Willet Road
Buffalo, NY 14218

266. Michael A. Rigdon
Institute for Defense
Analyses
1801 Beauregard Street
Alexandria, VA 22=11

267. John E. Ritter, Jr.
University of Massachusetts
Mechanical Engineering
Department
Amherst, MA 01003

268. Giulio A. Rossi
Norton Company
High Performance Ceramics
Goddard Road
Northboro, MA 01532-1545

269. Barry R. Rossing
Aluminum Company of America
Alcoa Technical Center
Alcoa Center, PA 15069

270. David J. Rowcliffe
SRI International
Menlo Park, CA 94025

271. Donald W. Roy
Manager, Carbide and
Optical Material
Research and Development
Golden, CO 80401

272. Bruce Rubinger
50 Milk Street, 15th Floor
Boston, MA 02109

273. Robert Ruh
Air Force Wright
Aeronautical Laboratory
Materials Laboratory
AFWAL/MLLM
Metals and Ceramics
Division
Wright-Patterson AFB,
OH 45433

274. Robert J. Russell, Sr.
Divisional Vice President
Technology and Planning
High Performance Ceramics
Norton Company
Goddard Street
Northboro, MA 01532-1545

275. George P. Safol
Westinghouse Electric
Corporation
R&D Center
Pittsburgh, PA 15235

276. J. Sankar
North Carolina Agricultural and Technical State University
Department of Mechanical Engineering
Greensboro, NC 27411

277. Maxine Savitz
Assistant to Vice President, Engineering
The Garrett Corporation
PO Box 92248
Los Angeles, CA 90009

278. Richard Schapery
Texas A&M University
Civil Engineering Department
College Station, TX 77843

279. J. L. Schienle
Garrett Turbine Engine Company
111 S. 34th Street
Phoenix, AZ 85034

280. L. J. Schioler
Aerojet Tech Systems Company
PO Box 13222
Dept. 9990, Bldg. 2001
Sacramento, CA 95813

281. Arnie Schneck
Deere and Company
PO Box 128
Wood-Ridge, NJ 07075

282. Matthew Schreiner
Gas Research Institute
8600 W. Bryn Mawr Avenue
Chicago, IL 60631

283. John Schuldies
Industrial Ceramic Technology, Inc.
141 Enterprise Drive
Ann Arbor, MI 48103

284. R. B. Schulz, Manager
Advanced Materials Development
Office of Transportation Systems
Department of Energy
Forrestal Building CE-151
1000 Independence Avenue
Washington, DC 20585

285. Wesley J. C. Schuster
President
Thermo Electron Corporation
Metals Division
115 Eames Street
PO Box 340
Wilmington, MA 01887

286. Murray A. Schwartz
Bureau of Mines
2401 Eye Street, NW
Washington, DC 20241

287. Douglas B. Schwarz
Dow Chemical U.S.A.
52 Building
Midland, MI 48674

288. Thomas M. Sebestyen
U.S. Army Tank-Automotive Command
AMSTA-RGRT
Warren, MI 48397-5000

289. Brian Seegmiller
Senior Development Engineer
Coors Porcelain Company
17750 North 32 Street
Golden, CO 80401

290. S. G. Seshadri
Research Associate
Standard Oil Engineered Materials Company
Niagara Falls R&D Center
PO Box 832
Niagara Falls, NY 14302

291. Peter T. B. Shaffer
Executive Vice President
Advanced Refractory Technologies, Inc.
699 Hertel Avenue
Buffalo, NY 14207

292. Maurice E. Shank
Director, Engineering Technology Assessment
United Technologies Corporation
Pratt and Whitney Engrg. Div.
MS 162-31
East Hartford, CT 06108

293. Laurel M. Sheppard
Associate Editor
Advanced Materials and Processes
Route 87
Metals Park, OH 44073

294. Dinesh K. Shetty
The University of Utah
Dept. of Materials Science and Engineering
Salt Lake City, UT 84112

295. Jack D. Sibold
Coors Porcelain Company
17750 North 32 Street
Golden, CO 80401

296. Neal Sigmon
Appropriations Committee
Subcommittee on Interior and Related Events
U.S. House of Representatives
Rayburn Building, Room B308
Washington, DC 20515

297. Richard Silberglitt
DHR, Inc.
6849 Old Dominion Drive
Suite 228
McLean, VA 22101

298. Maurice J. Sinnott
University of Michigan
Chemical and Metallurgical Engineering
438 W. Engineering Building
Ann Arbor, MI 48109

299. S. R. Skaggs
Los Alamos National Laboratory
PO Box 1663
MS F-682, Program Office
Los Alamos, NM 87545

300. J. Thomas Smith
Director, Precision Materials Tech.
GTE Laboratories, Inc.
40 Sylvan Road
Waltham, MA 02254

301. Jay R. Smyth
Senior Development Specialist
Garrett Turbine Engine Company
PO Box 5217
MS 93-172/1302-2K
Phoenix, AZ 85010

302. Rafal Sobotowski
Standard Oil Engineered Materials
Research and Development
3092 Broadway Avenue
Cleveland, OH 44115

303. Boyd W. Sorenson
E. I. DuPont de Nemours & Company
Textile Fibers Dept. - E304C123
Wilmington, DE 19898

304. Richard M. Spriggs
National Materials Advisory Board
National Research Council
2101 Constitution Avenue
Washington, DC 20418

305. John D. Spuller
Division Manager
Government Products
Deere and Company
John Deere Road
Moline, IL 61265

306. M. Srinivasan
Standard Oil Engineered Materials
Niagara Falls R&D Center
PO Box 832
Niagara Falls, NY 14302

307. Gordon L. Starr
Manager, Metallic/Ceramic Materials Dept.
Cummins Engine Company, Inc.
Box 3005, Mail Code 50183
Columbus, IN 47202-3005

308. Harold L. Stocker
Manager, Low Heat Rejection Program
General Motors Corporation
Allison Gas Turbine Operations
PO Box 420, T-23
Indinapolis, IN 46206-0420

309. Roger Storm
Director, Niagara Falls R&D Center
Standard Oil Engineered Materials Company
PO Box 832
Niagara Falls, NY 14302

310. E. E. Strain
Program Manager AGT-101
Garrett Turbine Engine Company
111 S. 34th Street
PO Box 5217, Mail Stop 301-2N
Phoenix, AZ 85010

311. Thomas N. Strom
NASA Lewis Research Center
21000 Brookpark Road, 77-6
Cleveland, OH 44135

312. Paul Sutor
Midwest Research Institute
425 Volker Blvd.
Kansas City, MO 64116

313. J. J. Swab
U.S. Army Materials Technology Laboratory
Arsenal Street
Watertown, MA 02172

314. Lewis Swank
Ford Motor Company
PO Box 2053
Building SRL, Room E3172
Dearborn, MI 48121

315. Anthony C. Taylor
Staff Director
Subcommittee on Transportation, Aviation, & Materials
Committee on Science and Technology
U.S. House of Representatives
Rayburn Building, Room 2321
Washington, DC 20515

316. W. H. Thielbahr
Chief, Energy Programs Branch
Department of Energy
Idaho Operations Office
550 2nd Street
Idaho Falls, ID 83401

317. Earl Thompson
Assistant Director
United Technologies Corporation
Research Center
Silver Lane
East Harford, CT 06108

318. John K. Tien
Director of Center for Strategic Materials
Columbia University
1137 SW Mudd Building
New York, NY 10027

319. T. Y. Tien
University of Michigan
Materials and Metallurgical Engineering
Dow Building
Ann Arbor, MI 48109-2136

320. Julian M. Tishkoff
Research
Directorate of Aerospace Sciences
Bolling AFB
Washington, DC 20332

321. Maurice L. Torti
Senior Scientist, High Performace Ceramics
Norton Company
Goddard Road
Northboro, MA 01532-1545

322. Louis E. Toth
National Science Foundation
Division of Materials Research
1800 G Street, NW
Washington, DC 20550

323. Richard E. Tressler
Chairman, Ceramic Science and Engineering Department
The Pennsylvania State University
201 Steidle Building
University Park, PA 16802

324. Donald R. Uhlmann
Professor, Ceramics and Polymers
Department of Materials Science and Engineering
Massachusetts Institute of Technology
Cambridge, MA 02139

325. Thomas Vasilos
Manager, Electro Chemical Facility
Avco Corporation
201 Towell Street
Wilmington, MA 01887

326. V. Venkateswaran
Standard Oil Engineered Materials Company
PO Box 832
Niagara Falls, NY 14302

327. John B. Wachtman, Jr.
Director, Center for Ceramics Research
Rutgers University
PO Box 909
Piscataway, NJ 08854

328. Richard B. Wallace
Manager, Government Research and Development Programs
General Motors Corporation
Detroit Diesel Allison Division
36880 Ecorse Road
Romulus, MI 48174

329. Harlan L. Watson
Subcommittee on Energy Research and Production
U.S. House of Representatives
Committee on Science and Technology
Rayburn Building
Suite 2321
Washington, DC 20515

330. Steven G. Wax
Department of Defense
Advanced Research Projects Agency
Materials Science Division
1400 Wilson Boulevard
Arlington, VA 22209

331. Albert R. C. Westwood
Corporate Director, R&D
Martin Marietta Laboratories
1450 South Rolling Road
Baltimore, MD 21227

332. Thomas J. Whalen
Principal Research Scientist
Ford Motor Company
Scientific Lab, Room 2023

333. Sheldon M. Wiederhorn
U.S. Department of Commerce
National Bureau of Standards
Inorganic Materials Division
Mechanical Properties Group
Gaithersburg, MD 20899

334. Roger R. Wills
Manager, Advanced Ceramic Components
TRW, Inc.
Automotive Worldwide Sector
Valve Division
Cleveland, OH 44110

335. J. M. Wimmer
Supervisor, Nonmetallic Materials Group
Garrett Turbine Engine Company
111 S. 34th Street, PO Box 5217
Phoenix, AZ 85010

336. David Wirth
Vice President, Technical Operations & Engineering
Coors Porcelain Company
17750 North 32 Street
Golden, CO 80401

337. Thomas J. Wissing
Manager, Government Contract Administration
Eaton Corporation
Engineering & Research Center
26201 Northwestern Highway
PO Box 766
Southfield, MI 48037

338. George W. Wolter
Howmet Turbine Components Corporation
Technical Center
699 Benston Road
Whitehall, MI 49461

339. James C. Wood
NASA Lewis Research Center
21000 Brookpark Road, MS 500-21
Cleveland, OH 44135

340. Hun C. Yeh
Ceramic Supervisor
AiResearch Casting Company
19800 Van Ness Avenue
Torrance, CA 90509

341. Thomas M. Yonushonis
Cummins Engine Company, Inc.
Box 3005, Mail Code 50183
Columbus, IN 47202-3005

342. Don Zabierek
Air Force Wright Aeronautical Laboratory
AFWAL/POTC
Wright-Patterson AFB, OH 45433

343. Charles Zeh
Department of Energy
Morgantown Energy Technology Center
PO Box 880
Morgantown, WV 26505

344. Klaus M. Zwilsky
Executive Director
National Materials Advisory Board
National Research Council
2101 Constitution Avenue
Washington, DC 20418

345. Department of Energy
Oak Ridge Operations Office
Assistant Manager for Energy Research and Development
PO Box E
Oak Ridge, TN 37831

346–375. Department of Energy
Technical Information Center
Office of Information Services
PO Box 62
Oak Ridge, TN 37831

For distribution by microfiche as shown in DOE/TIC-4500, Distribution Category UC-95

☆ U.S. GOVERNMENT PRINTING OFFICE 1987—748—168/40146